



Published in final edited form as:

Circ Cardiovasc Genet. 2016 December ; 9(6): 474–486. doi:10.1161/CIRCGENETICS.116.001515.

Sucrose Non-Fermenting Related Kinase Enzyme Mediated Rho-Associated Kinase Signaling is Responsible for Cardiac Function

Stephanie M. Cossette, PhD¹, Vijesh J. Bhute, BTech³, Xiaoping Bao, PhD³, Leanne M. Harmann, BA², Mark A. Horswill, MS⁴, Indranil Sinha, PhD⁵, Adam Gastonguay, PhD¹, Shabnam Pooya, PhD¹, Michelle Bordas, BS¹, Suresh N. Kumar, PhD⁶, Shama P. Mirza, PhD⁸, Sean Palecek, PhD³, Jennifer Strande, MD, PhD⁷, and Ramani Ramchandran, PhD^{1,9}

¹Department of Pediatrics, Medical College of Wisconsin, Developmental Vascular Biology Program, Children's Research Institute, Milwaukee

²Division of Cardiovascular Medicine, Cardiovascular Center, Clinical and Translational Science Institute, Medical College of Wisconsin, Milwaukee

³Department of Chemical and Biological Engineering, University of Wisconsin-Madison, Madison, WI

⁴Morgridge Institute for Research, University of Wisconsin-Madison, Madison, WI

⁵Marginalen Bank, Stockholm, Sweden

⁶Division of Pediatric Pathology, Department of Pathology, Medical College of Wisconsin, Milwaukee

⁷Division of Cardiovascular Medicine, Department of Cell Biology, Neurobiology and Anatomy, Cardiovascular Center, Clinical and Translational Science Institute, Medical College of Wisconsin, Milwaukee

⁸Department of Chemistry and Biochemistry, University of Wisconsin-Milwaukee, Milwaukee, WI

⁹OBGYN, Medical College of Wisconsin, Developmental Vascular Biology Program, Children's Research Institute, Milwaukee

Abstract

Background—Cardiac metabolism is critical for the functioning of the heart, and disturbance in this homeostasis is likely to influence cardiac disorders or cardiomyopathy. Our lab has previously shown that sucrose non-fermenting related kinase (SNRK) enzyme, which belongs to the AMP-activated kinase (AMPK) family, was essential for cardiac metabolism in mammals. *Snrk* global homozygous knockout (KO) mice die at postnatal day 0, and conditional deletion of *Snrk* in cardiomyocytes (*Snrk* cmcKO) leads to cardiac failure, and death by 8–10 months.

Correspondence: Ramani Ramchandran, PhD, Department of Pediatrics, Medical College of Wisconsin, CRI Developmental Vascular Biology Program, C3420, 8701 Watertown Plank Road, P.O. Box 26509, Milwaukee, WI 53226, Tel: 414-955-2387, Fax: 414-955-6325, rramchan@mcw.edu.

Disclosures: None

Methods and Results—We performed additional cardiac functional studies using echocardiography (ECHO), and identified further cardiac functional deficits in *Snrk* cmcKO mice. NMR-based metabolomics analysis identified key metabolic pathway deficits in *SNRK* knockdown cardiomyocytes (CMs) *in vitro*. Specifically, metabolites involved in lipid metabolism and oxidative phosphorylation are altered and perturbations in these pathways can result in cardiac function deficits and heart failure. A phosphopeptide-based proteomic screen identified Rho-associated kinase (ROCK) as a putative substrate for SNRK and mass spec-based fragment analysis confirmed key amino acid residues on ROCK that are phosphorylated by SNRK. Western blot analysis on heart lysates from *Snrk* cmcKO adult mice and *SNRK* knockdown CMs showed increased ROCK activity. In addition, *in vivo* inhibition of ROCK partially rescued the *in vivo* *Snrk* cmcKO cardiac function deficits.

Conclusions—Collectively, our data suggests that SNRK in CMs is responsible for maintaining cardiac metabolic homeostasis, which is mediated in part by ROCK and alteration of this homeostasis influences cardiac function in the adult heart.

Keywords

metabolism; cardiac; Rho-associated kinases; echocardiography; SNRK; MYH6

Introduction

Cardiomyopathy is a complex disorder influenced by several factors. Some of these factors include impaired endothelial function and sensitivity to various ligands (β -agonists), altered intracellular calcium homeostasis, and accumulation of connective tissue such as insoluble collagen¹. Recently, cardiomyopathy as a consequence of early alterations in cardiac metabolism has been proposed, particularly with respect to diabetes². A potential link between cardiac metabolism and function is the Ras homolog family member A (RhoA)-associated kinase (ROCK) signaling pathway. The RhoA/ROCK signaling pathway has been implicated in several cardiovascular and metabolic disorders such as atherosclerosis, cardiac hypertrophy and diabetes³. ROCK is a serine threonine kinase involved in regulating various cellular processes such as cell contraction, migration, proliferation, apoptosis/survival and gene expression/differentiation⁴. Interestingly, pharmacological inhibition of RhoA/ROCK activity has been shown to improve cardiac function in diabetes-induced cardiomyopathy⁵. To date signaling molecules regulating ROCK activity have primarily been restricted to the RhoA pathway. Our lab has identified a novel member of the AMP-activated kinase (AMPK) family namely sucrose non-fermenting related kinase (SNRK) that is essential for angiogenesis⁶, and responsible for cardiac metabolism in mammals⁷. Here, we implicate SNRK as a putative regulator of ROCK activity in cardiomyocytes (CMs).

CMs metabolism is developmentally dynamic in that the fetal heart primarily utilizes glucose as its major energy substrate, and during postnatal maturation, the heart switches to primarily utilizing fatty acid oxidation to meet its energy demands^{8, 9}. In our previous work⁷, we reported that the global *Snrk* KO mice die within 24 hours after birth, displayed enlarged hearts, and lethality is associated with metabolic defects in cardiac tissues. SNRK maintains metabolic homeostasis via regulation of the phosphorylated acetyl-coA carboxylase (pACC)-phosphorylated AMPK (pAMPK) pathway during this transitional

period in development⁷. Furthermore, cardiac specific conditional *Snrk* KO (*Snrk* cmcKO) adult mice display severe cardiac functional deficits and lethality within 8–10 months. We extend this work further in this study, and identified ROCK as a putative substrate for SNRK that contributes to this metabolic deficit in the heart. NMR-based metabolomics in human embryonic stem cell derived-CMs and signaling studies in both adult heart lysates and cultured CMs collectively imply that SNRK-mediated ROCK signaling pathway is an important regulator of cardiac function in mammals.

Methods

Detailed methods are described in the Supplemental Materials.

Fasudil Rescue

Male and female mice between six and four months of age were given fasudil (10mg/kg) or saline daily for 28 days via intraperitoneal injections. ECHO analysis was performed immediately prior to the initial injection and ECHO imaging was repeated at 14 and 28 days. At the end of the experiment the mice were euthanized using CO₂ and cervical dislocation as per the approved IACUC animal protocol.

Metabolomics Analysis

CMs treated with either non-silencing shRNA control or shSNRK lentivirus were cultured in RPMI containing B27 (no insulin) for 48 h prior to sample collection. Sample collection and extraction was performed as described previously in Bhute and Palecek¹⁰. ¹H NMR spectra were acquired using standard NOESYPR1D pulse sequence (RD-90°-t1-90°-tm-90°-acquire) with a relaxation delay of 1 s, a mixing time of 100 ms and a pre-scan delay of 30 μs and consisted of 128 transients or free induction decays (FIDs) collected into 48 K complex data points with a spectral width of 12 ppm and an acquisition time of 4 s. FIDs were zero-filled to 128k data points and multiplied by an exponential window function (LB=0.5Hz). The chemical shifts were referenced to the TMS peak (δ=0 ppm), using TopSpin™ software (version 3.1, Bruker). Spectral processing like phasing, baseline correction and solvent region removal (water and DMSO) was performed using ACD/1D NMR processing (Advanced Chemistry Development). Targeted profiling¹¹ was performed using ChenomX NMR Suite Profiler (version 7.7, ChenomX Inc.) and the concentrations were references to TMS. Peak annotation was performed based on the existing ChenomX library and HMDB¹². The metabolite concentrations were exported to an Excel file for further analysis.

The concentration data matrix was normalized by the total concentration of metabolites, which was equivalent to normalization by total spectral area in each sample to evaluate the metabolite fractions and also to account for the differences in cell number and efficiencies of extraction. Statistical and pathway analysis was performed using MetaboAnalyst 3.0¹³. The concentration data was auto-scaled (mean centering followed by dividing each variable by the standard deviation) prior to principal component analysis (PCA) and student's t-test was performed assuming unequal group variance and α was chosen to be 0.05. Pathway topology analysis was performed in MetaboAnalyst's pathway analysis module using global test

algorithm for pathway enrichment (adjusted for multiple testings) and out-degree centrality to assess importance. The *Homo Sapiens* library was used for analysis and the metabolic pathways with an impact score > 0 and FDR<0.05 were considered to be significantly enriched.

Protein Kinase Array

Purified SNRK protein was provided to Invitrogen (Life Technologies) for kinase substrate identification service on ProtoArray human protein microarray. In short, SNRK was assayed at concentration of 5 nM and 50 nM on ProtoArray human protein microarrays v5.0. All possible kinase substrates at each concentration of SNRK were evaluated by their Z-Factor rank within the array and were compared to the negative control assay. A protein was defined as being a candidate substrate if it met the following conditions: The Z-Factor, or signal-to-noise ratio, was great than 0.35 on at least one array, indicating a signal greater than 1.5-fold above the noise. The Signal Used value was greater than 2,000 relative units on at least one array probed with SNRK and was greater than 2-fold higher than the Signal Used value for the corresponding protein in the negative control assay. The replicate spot CV was less than 50% on the corresponding array. The inter-assay CV was less than 50%. Additional experimental details are available upon request.

In vitro ROCK Phosphorylation Protocol

Human umbilical vein endothelial cells (HUVECs) (Lonza CC2519) were lysed with RIPA buffer (Sigma) containing complete mini EDTA-free protease inhibitor cocktail (Roche) and PhosSTOP phosphatase inhibitor (Roche). Samples were incubated on ice for 20 mins and cleared at 13,300 rpm at 4°C for 30 mins. ROCK1 was immunoprecipitated using an anti-ROCK1 antibody (Cell Signaling Technology) with protein G agarose beads (Thermo Scientific). Immunoprecipitates were washed 3× with dilution buffer (10 mM Tris, 130 mM NaCl, 0.05% Triton-X-100, 0.1% BSA, protease inhibitors). Additional washes with 50 mM Tris (pH 8.0) and Tris-Saline (10 mM Tris HCl, 140 mM NaCl) (pH 8.0) were also performed. The Lowry quantification method was used to determine the protein concentration. Immunoprecipitated ROCK1 protein was incubated with or without 5 nM to 30 nM purified SNRK protein in the presence of 3 μM γ-ATP-32 (Perkin Elmer) and 1 μM ATP (Cell Biolabs) in kinase buffer [20 mM HEPES (pH7.7), 20 mM MgCl₂, 2 mM DTT, 1X protease inhibitor (Roche) and 1X phosphatase inhibitor (Roche)]. The samples were allowed to incubate for 15 mins at 30°C. After incubation the samples were washed 2–3 times with kinase buffer and re-suspended in Lamelli sample buffer. 5 μl of the reaction was reserved for radioactive analysis and the remaining samples were resolved on a 10% Mini-PROTEAN TGX precast gel (BioRad) and subjected to SDS-PAGE. The gel was then dried and exposed to autoradiography film.

Western Blot (WB) Analysis

Adult heart tissues were collected immediately after euthanization, and the proteins were isolated using homogenization in RIPA buffer (Sigma) with complete mini EDTA-free protease inhibitor cocktail (Roche) and PhosSTOP phosphatase inhibitor (Roche) using a Qiagen TissueRuptor. Methodologies related to protein estimation, quantitation were described previously⁷. The following antibodies were used: anti- myosin-binding subunit

(MBS; BioLegend), anti-phospho MBS (pMBS; Cell Signaling Technology/MBL International); anti-ROCK1 (BD Bioscience); anti-ROCK2 (BD Bioscience); anti-extracellular signal-regulated kinase (ERK; Cell Signaling Technology); anti-phospho ERK (pERK; Cell Signaling Technology); anti-protein kinase B (AKT; Cell Signaling Technology); anti-phospho AKT (pAKT; Cell Signaling Technology); anti-inhibitor of kappa B kinase (IKK; Cell Signaling Technology); anti-phospho IKK (pIKK; Cell Signaling Technology); anti-Tubulin (Sigma), anti-rabbit horseradish peroxidase (HRP; Cell Signaling Technology) and anti-mouse HRP (Cell Signaling Technology).

Statistics

Student's unpaired t-test was used for comparison analysis for the cardiomyocyte western blot, metabolomics and trichrome staining analysis. Mann-Whitney test was used for comparison analysis for the adult heart western blot analysis and all of the ECHO data analysis. The results are described as means (\pm standard error of the mean, SEM). A p-value of $p < 0.1$ was considered to be approaching significance. A p-value of $p < 0.05$ was considered significant when comparing two parameters. For all of the *in vivo* and *in vitro* ROCK signaling and inhibitor experiments a p-value of $p < 0.05$ was considered to be slightly significant, and a p-value of $p < 0.0125$ was considered significant due to p-value correction for multiple comparisons. Sample data values for the trichrome staining analysis and the western blot experiments are provided in Table S1. Sample data values for the metabolomics data are provided in Table S2.

Results

***Snrk* cardiac (cmcKO) conditional knockout adult mice show myocardial dysfunction and increased cardiac fibrosis**

Previously, our lab assessed the role of *Snrk* in mammalian development, and concluded that SNRK is essential for cardiac metabolism⁷. In that study, we generated and validated the global and cardiac-specific (MYH6CRE)¹⁴ conditional *Snrk* cmcKO mouse reagents⁷. Homozygous loss of *Snrk* (LoxP/LoxP) in CMs results in lethality between 8–10 months of age and heterozygous loss of *Snrk* (LoxP/WT) showed lethality shortly after one year of age. Echocardiography (ECHO) analysis on 6 month old adult male mice showed significant enlargement of the left ventricle inner diameter (LVID) in systole (s) and diastole (d), significant increase in end diastolic volume (EDV) and end systolic volume (ESV), significant decrease in the ejection fraction (EF) and the fractional shortening (FS) in the *Snrk* cmcKO (MYH6CRE *Snrk*^{LoxP/LoxP}) mice compared to the CRE negative littermates⁷. We now performed strain and strain rate imaging analysis (Fig. 1A), which showed that *Snrk* cmcKO display significantly worsening strain patterns including decreased radial strain ($p = 0.0286$), increased circumferential strain ($p = 0.0286$), decreased strain rates S ($p = 0.0286$). The strain rate changes correlates with a decrease in systolic function. The *Snrk* cmcKO mice also display an increased strain rate E ($p = 0.0286$) that is associated with worsening diastolic function. Furthermore, the pulmonary acceleration time (PAT) ($p = 0.0571$), ejection time (ET) ($p = 0.0571$) (Fig. 1B) and right ventricular outflow tract time velocity-integrals (TVI) were also decreased in *Snrk* cmcKO ($p = 0.0571$) (Fig. 1C). All together, these findings

are consistent with a dilated cardiomyopathy with a resultant increase in pulmonary artery pressure.

We next investigated whether myocardial stiffening and impaired cardiac function could be the result of increase in extracellular matrix deposition, a phenomenon described as myocardial fibrosis¹⁵. We performed trichrome staining on *Snrk* cmcKO heart tissue sections (Fig. 1D). *Snrk* cmcKO showed a significant increase in fibrosis staining (CRE neg 10.38%, cmcKO 19.32% p=0.0212) (Fig. 1E and Table S1). These data indicates deformation in the heart segments resulting in altered myocardial function and suggest that *Snrk* in CMs is critical for maintaining heart contractility.

SNRK knockdown CMs *in vitro* show defective metabolism

To investigate what might be amiss in CMs in the absence of SNRK, we investigated changes in metabolism in *SNRK* knockdown CMs *in vitro* since previous data on *Snrk* cmcKO mice showed cardiac metabolic defects⁷. CMs treated with either non-silencing shRNA control or efficacy-confirmed shSNRK lentivirus was subjected to NMR-based metabolomics measurement as described in the methods section. The heat maps (Fig. 2A) and subsequent graphical representation (Fig. 2B) clearly depict extensive metabolic changes in *SNRK* knockdown CMs. Metabolites that significantly increased (Fig. S1A) and decreased (Fig. S1B) in *SNRK* knockdown CMs have been indicated. Among the increased metabolites, we observed significant increase in multiple osmolytes including glycerophosphocholine (Fold Change: 1.44, p=0.0046) and taurine (Fold Change: 1.27, p=0.038). We also observed an increase in a few essential amino acids including valine and threonine while, majority of the non-essential amino acids including alanine (p<0.1), asparagine, aspartate, glutamate, and glutamine showed a significant decrease due to *SNRK* knockdown (p<0.05). This indicates significant changes in amino acid-related metabolic pathways, which is also observed in pathways analysis (Fig. 2C). Interestingly, glycerol was significantly increased due to *SNRK* knockdown relative to control (Fold Change: 1.38, p=0.018). Glycerol can serve as substrate for energy in cardiomyocyte¹⁶ and we observe several other metabolites associated with energy metabolism including citrate, fumarate, malate, succinate (p<0.05), pyruvate and NAD (p<0.1) to be significantly reduced due to *SNRK* knockdown in CMs. This indicates that SNRK can play a crucial role in energy homeostasis in CMs.

Further pathway topology analysis (Fig. 2C) and metabolite set enrichment analysis (Fig. 2D) suggested significant changes in alanine, aspartate and glutamate metabolism (p=0.002) (Fig. 2C and S2), citrate cycle (p=3.47E-06) (Fig. 2C and S3), taurine and hypotaurine metabolism (p=0.002), aminoacyl t-RNA biosynthesis (p=0.009) and glycine, serine and threonine metabolism (p=0.01) (Fig. 2C). Specific metabolites and amounts that changed in *SNRK* knockdown CMs are indicated in supplemental Tables S2 and S3. Taking the *in vivo* and *in vitro* data together, SNRK in CMs plays an instrumental role in maintaining metabolic homeostasis, which is critical for the normal functioning of the heart.

ROCK is a putative substrate of SNRK

To identify signaling proteins responsible for the cardiac function deficits observed in *Snrk* cmcKO mice *in vivo*, we performed a phosphopeptide proteomic screen using pure SNRK protein generated in the lab. Human histidine tagged SNRK protein was generated in bacteria (Fig. S4), purified (Fig. S4A), and confirmed by mass spectral (MS) analysis (23% peptide coverage) and western blotted for SNRK antibody (Fig. S4D). Using this purified SNRK protein (Fig. S4E), we outsourced the kinase profiling to Life Technologies. An *in vitro* protein kinase experiment was performed on 9,000 N-terminal GST fusion proteins on an array at two SNRK protein concentrations (5 and 50 nM). This screen identified Rho-associated kinase 1 (ROCK1) as one of the top hits along with several members of the transforming growth factor- β (TGF- β) signaling pathway (ACVR1, ACVRL1, SMAD3, BMPR2) that showed 2-fold or more phosphorylation compared to negative control (Table. S4). We confirmed the ROCK1 phosphorylation *in vitro* using a ROCK kinase assay (Fig. 3A). ROCK1 protein was immunoprecipitated (IPed) from human umbilical vein endothelial cells (HUVECs) (Fig. 3A, IP blot), and was incubated with purified SNRK protein in the presence of radiolabeled phosphate (P^{32}). As shown (Fig. 3A, lane 2), a P^{32} -labeled band is observed in the lane with IPed ROCK plus SNRK protein at the correct size for the ROCK1 protein, which was quantified in three independent experiments (Fig. 3A, Quantitation panel). In addition, we performed multi-stage fragmentation tandem Mass Spectrometry on ROCK1 IPed from HUVECs in the presence or absence of SNRK. The ROCK1 band was excised and subjected to in-gel tryptic digestion. The resulting peptides were analyzed by multi-stage fragmentation mass spectral analysis¹⁷. The data for ROCK1 identified residues S27, T237, S479 (Fig. S5, blue circles) that resides in the N-terminal region. These sites are distinct from those reported in the literature (Fig. S5 magenta circles) or previously identified using proteomic approaches (Fig. S5, yellow highlighted residues). Collectively, this data suggests that ROCK1 is a direct target of SNRK, and phosphorylation of ROCK by SNRK at specific residues is likely to influence its downstream activity.

We next evaluated ROCK activity by determining the amount of phospho-Threonine 853 in the myosin-binding subunit (pMBS) of myosin light chain phosphatase, a key enzyme in the RhoA-ROCK muscle contraction signaling cycle. We performed western blots for ROCK1, ROCK2 and pMBS protein levels in *Snrk* cmcKO adult (Fig. 3B) heart lysates. Of the proteins investigated, pMBS levels were higher in adult *Snrk* cmcKO hearts (MYH6CRE SNRK L/L) (Fig. 3B, $p=0.1$) compared to CRE negative controls. We also investigated SNRK knockdown CMs *in vitro* for pMBS, and observed an increase that was not significant (Fig. 4A, $p=0.36$, $n=3$). Interestingly, when control and shSNRK knockdown CMs were treated with the ROCK inhibitor Y27632 (Fig. 4A), there was a slightly significant decrease in pMBS levels compared to control treated shSNRK knockdown CMs (40.75% $p=0.041$, $n=3$). Specific sample data values are indicated in supplemental Tables S1. Collectively, the phosphoproteomic analysis and signaling data suggests that ROCK is a substrate of SNRK, and ROCK activity is attenuated by SNRK *in vivo* and *in vitro* in CMs.

SNRK-ROCK signaling in cardiomyocytes

We next investigated signaling pathways that can be regulated by ROCK signaling such as protein kinase b alpha (AKT) and mitogen-activated protein kinase (ERK) in both *in vivo*

Snrk cmcKO mice (Fig. 3B), and *in vitro* SNRK knockdown CMs (Fig. 4B–D). ROCK is known to regulate the phosphoinositide 3-kinase (PI3K)-AKT pathway by activating the phosphatidylinositol (3,4,5)-trisphosphate (PIP3) phosphatase called phosphatase and tensin homolog (PTEN), which results in a reduction in pAKT levels^{18, 19}. In addition, ROCK has also been shown to influence ERK signaling in smooth muscle cells²⁰. Western blot analysis was conducted on *Snrk* WT and cmcKO hearts lysates as well as control and shSNRK knockdown cells with and without the ROCK inhibitor Y27632. Loss of SNRK in the heart resulted in decreased pAKT (Fig. 3B, 46.15%, $p=0.1$, $n=3$) and the AKT downstream effector pIKK (Fig. 3B, 44.62%, $p=0.1$, $n=3$), which suggests decreased AKT signaling in the *Snrk* cmcKO hearts. We also observed a trend towards increased pERK (Fig. 3B, 183.47%, $p=0.2$, $n=3$) in the heart lysates. Specific sample data values are indicated in supplemental Tables S1.

Surprisingly knockdown of SNRK in CMs resulted in a non-significant change in pAKT (Fig. 4B, 171.07%, $p=0.136$, $n=4$) and pERK (Fig. 4D, 311.64%, $p=0.212$), and a significant increase in pIKK (Fig. 4C, 254.38%, $p=0.012$, $n=3$). Inhibition of ROCK signaling using the ROCK inhibitor Y27632 was able to significantly decrease the pMBS levels in the shSNRK CM compared to the control treated shSNRK CM (Fig. 4A, Control 123.35%, shSNRK 40.75% $p=0.041$, $n=3$). pAKT, pERK and pIKK levels did not significantly change in the presence of the ROCK inhibitor (Fig. 4C) suggesting that ROCK signaling is not the only molecule involved in regulating pAKT, pERK and pIKK signaling in cultured CMs. These results collectively suggest that SNRK directly influences ROCK signaling in CMs *in vivo* and *in vitro*.

SNRK-ROCK signaling is required for normal cardiac function

Altered ROCK signaling has been previously implicated cardiac hypertrophy and ventricular remodeling^{4, 21, 22}. To determine whether the cardiac defects observed in the *Snrk* cmcKO mice are attributed to increased ROCK activation, *Snrk* WT and *Snrk* cmcKO mice were treated with the ROCK inhibitor fasudil²³. To assess changes in cardiac function, ECHO was conducted before drug treatment and after 4 weeks of daily fasudil or saline injection (Fig. 5 and Table S5). Fasudil treatment in *Snrk* cmcKO mice resulted in stabilization of EF and FS phenotypes, from 55.55% (cmcKO-Fasudil) and 50.66% (cmcKO-Saline) EF and 24.77%-22.7% FS before treatment to 53% EF and 23.23% FS after fasudil treatment compared to the saline treated *Snrk* cmcKO mice which displayed continued declines in EF (44.55% $p=0.0286$) and FS (18.9% $p=0.0286$). EDV did not show a significant change in the *Snrk* cmcKO mice (0.0064) treated with fasudil compared to baseline (0.0070, $p=0.6905$) whereas EDV continued to increase in the saline treated *Snrk* cmcKO mice from 0.0066 at baseline to 0.0082 at 4 week ($p=0.0286$). ESV did not increase in the fasudil treated *Snrk* cmcKO mice but did in the saline treated mice (baseline 0.0029 to 4 weeks 0.0046, $p=0.0286$) indicating a preserved EF in the fasudil treated mice. IVRT showed a similar trend with a slight decrease in the fasudil treated *Snrk* cmcKO mice (baseline 14.45 to 4 weeks 12.41, $p=0.3413$), and an increase in *Snrk* cmcKO saline treated mice (baseline 12.4 to 4 weeks 13.22, $p=0.0286$). These data indicates that increased ROCK activity is involved in generating the cardiac functional deficits observed in the *Snrk* cmcKO mice and that inhibition of ROCK results in cardiac functional improvements.

Discussion

In this study, we have identified that a member of the AMPK family namely SNRK influences ROCK signaling to maintain cardiac function in the adult. *Snrk* was first identified in 3T3-L1 differentiated adipocyte cells²⁴, and compared to *Ampka1* and *Ampka2*, *Snrk* expression in white adipose tissue, brown adipose tissue, heart and brain is significantly higher²⁵. The expression profile of SNRK, and the family that it belongs to suggest a role for this enzyme during high metabolic needs like the heart contraction and relaxation cycles. Indeed in our previous report⁷, we identified that SNRK is a critical regulator of metabolic function during embryonic cardiovascular development, and identified the metabolic pAMPK-pACC signaling pathway deregulation in the heart. These results directly support current NMR-based metabolomic analysis data in *SNRK* knockdown CMs, which shows decreased metabolites such as those involved in alanine, aspartate and glutamate metabolism (Fig. S2), as well as citric acid cycle metabolism (Fig. S3), and increases in metabolites involved in lipid synthesis such as glycerol (Fig S1)²⁶ which are processes directly influenced by pAMPK-pACC signaling^{27, 28}. Interestingly perturbations in cardiac metabolic output have been observed in patients with heart failure^{29, 30}. In normal hearts, the primary metabolic energy source is derived by lipid metabolism/fatty acid oxidation and in failing hearts the metabolic substrate changes to glucose metabolism³¹. Furthermore, accumulation of lipids (free fatty acids) in the failing heart can create additional metabolic stress by increasing energy uncoupling and proton leakage and decreasing energy production^{32, 33}. In the *SNRK* knockdown CMs, we did not observe any significant changes in glycolysis or glucose metabolism but we did observe significant alterations in oxidative phosphorylation and lipid metabolism indicating an important role for SNRK in cardiac metabolism and loss of SNRK can result in a phenotypes similar to those observed during cardiac failure. In addition, taurine and hypotaurine metabolism was found to be increased in the *Snrk* knockdown CMs indicating the activation of compensatory mechanisms to increased osmotic stress^{34, 35}, and further supporting the notion that SNRK is an important regulator of cardiac cellular homeostasis.

To assess the contribution of SNRK to cardiac function, we conditionally deleted *Snrk* in CMs *in vivo* using MYH6CRE¹⁴ mouse line. The *Snrk* cmcKO mice develop cardiomyopathy and die at 8–10 months of age⁷. The 6 months ECHO studies showed changes in left ventricular dimensions and decreased ventricular function consistent with a dilated cardiomyopathy. Left heart failure often result in increased pulmonary artery pressures and our ECHO-Doppler interrogation of right heart hemodynamics corroborate this relationship. These mice over time progressively show increased fibrosis and cardiac stiffening, phenotypes associated with dysregulated ROCK signaling^{36, 37}. Indeed, we identified two key molecules namely the TGF- β signaling pathway and ROCK signaling pathways in our SNRK substrate screen both of which have been implicated in cardiac stiffening and fibrosis³⁷. We posit that SNRK's involvement in the two signaling pathways may not be mutually exclusive since both have been implicated in CMs function previously. For example, TGF- β 3 and ALK2 regulate ROCK1 expression during valvuloseptal endocardial cushion formation³⁸, and up regulation of bone morphogenetic protein-2 (BMP-2), antagonized TGF- β 1/ROCK-enhanced cardiac fibrotic signal through activation of

Smurf1/Smad6 complex³⁷. In this study, we only focused on ROCK because of the overwhelming evidence suggesting ROCK as a cardiovascular risk factor³⁹, and its role in cardiovascular physiology and pathophysiology⁴.

ROCKs' are ubiquitously expressed proteins, and both isoforms ROCK1 and ROCK2 are expressed in the heart⁴⁰. Signaling mechanisms associated with contraction in the vascular smooth muscle cells (SMCs) in the heart are well studied for ROCK. Briefly, intracellular Ca²⁺ level increases through activated G-protein coupled receptors, which in turn stimulate downstream phosphorylation of myosin light chain kinase (MLCK) (activating), and phosphorylation of the myosin binding subunit (MBS also known as MYPT1) of myosin light chain phosphatase (MLCP) (inactivating). The exchange factor RhoA is the chief upstream activator of ROCK1 to date, and has been the established regulator of this pathway⁴, the net result of which is contraction of SMCs. Our studies suggest SNRK is a second player upstream of ROCK but whether the phosphorylation directly activates or inhibits ROCK activity or whether additional proteins along with SNRK are required for altered ROCK activity is currently unknown. Our data suggests that SNRK is a negative regulator of ROCK signaling, and loss of SNRK increases ROCK activity in CMs. Indeed loss of SNRK in *Snrk* cmcKO adult (6 months) mice showed higher levels of pMBS reinforcing the hypothesis that phosphorylation of ROCK1 by SNRK may be inhibitory (Fig. 3). The converse experiment would be the overexpression or gain of SNRK in cardiac tissue, which should decrease ROCK activity and consequences associated with it. The resulting phenotype would include improved cardiac function since ROCK1 is necessary for the transition from cardiac hypertrophy to failure⁴¹. Indeed two abstracts report that SNRK overexpression in the heart improves cardiac metabolic efficiency and response to myocardial ischemia^{42, 43}, which support our predictive hypothesis.

We also examined the activation status of additional downstream effectors of ROCK such as AKT and ERK and identified altered *in vivo* expression levels of pAKT and pERK further suggesting that ROCK activity are altered *in vivo* when SNRK is absent (Figs. 3 and 6). Interestingly, we did not see a significant difference in the *in vitro* expression levels of pAKT, pERK and pMBS in *SNRK* knockdown CMs. These observations could be attributed to the inherent differences between *in vitro* culturing conditions and *in vivo* responses that contain additional non-CM cell types influencing the experimental readout. Additional *in vitro* studies are necessary to specifically address these differences.

To assess whether attenuation of ROCK signaling in *Snrk* cmcKO mice is consequential, we treated *Snrk* cmcKO mice with the ROCK inhibitor fasudil²³. Prior to treatment, the *Snrk* cmcKO already displayed cardiac functional defects. After 4 weeks of treatment with the inhibitor the *Snrk* cmcKO mice began showing signs of improved cardiac function and stabilization of the phenotype compared to the untreated *Snrk* cmcKO mice that continued to show decreased cardiac function (Fig. 5 and Table S5). These findings suggest that some of the cardiac functional deficits observed in the *Snrk* cmcKO mice are most likely a result increased ROCK activity and that SNRK regulation of ROCK signaling in an important component of normal cardiac function.

In summary, our data suggests that an AMPK family member SNRK is a critical metabolic sensor in cardiac tissues, and directly influences ROCK signaling in CMs, effects that directly contribute to maintaining cardiac metabolic homeostasis and cardiac functional output in mammals.

Supplementary Material

Refer to Web version on PubMed Central for supplementary material.

Acknowledgments

We thank members of the Developmental Vascular Biology Program for their invaluable input and insight during the course of this study. We also thank Dmitry L. Sonin for assistance with the initiation of the mouse ECHO studies and the Children's Research Institute imaging core facilities for Hamamatsu slide scanner and visiofarm image analysis support and the Histology core for slide preparations. This publication was supported by the National Center for Advancing Translational Sciences, National Institutes of Health, through Grant Number UL1TR001436. Its contents are solely the responsibility of the authors and do not necessarily represent the official views of the NIH.

Sources of Funding: S.M.C., S.P., A.G., M.B., and R.R. are supported in part by funds from NIH grants HL102745 and HL112639, and Women's Health Research Program at MCW. J.S is supported by NIH grant HL111148 and S.P., V.J.B. and X.B. are supported by NIH grant EB007534.

Reference

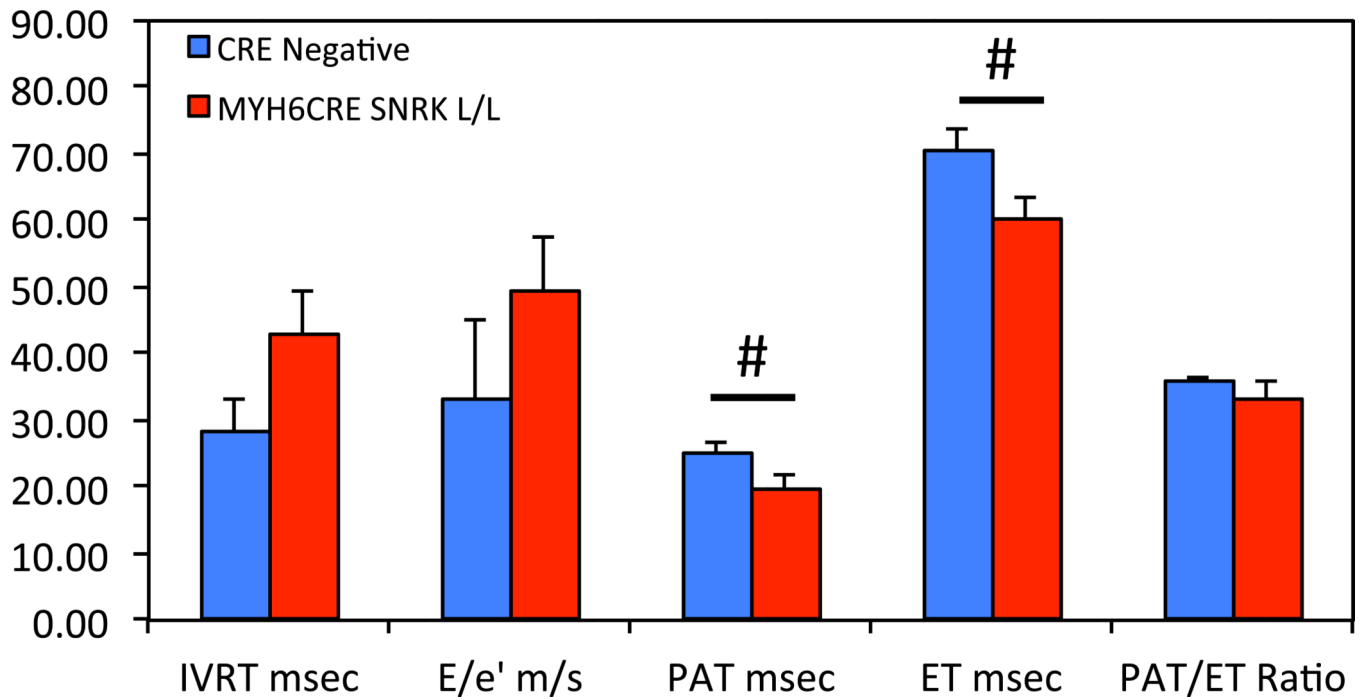
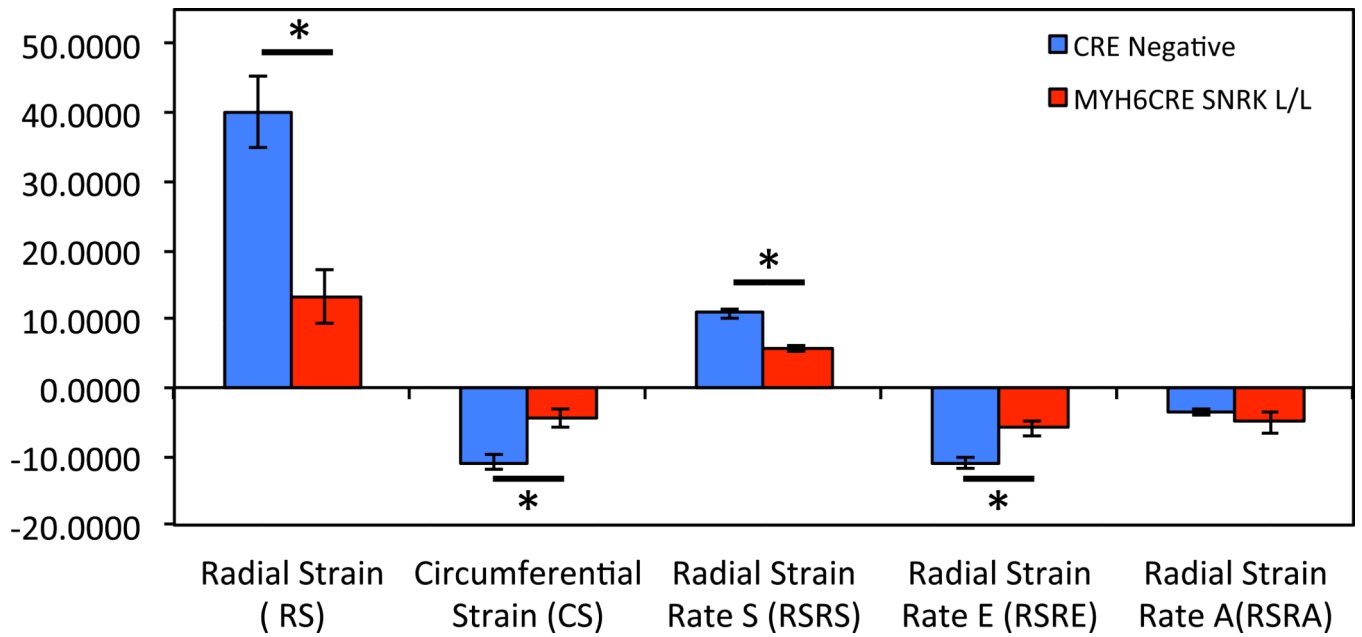
1. Alfieri O, Mayosi BM, Park SJ, Sarrafzadegan N, Virmani R. Exploring unknowns in cardiology. *Nat Rev Cardiol.* 2014; 11:664–670. [PubMed: 25245833]
2. Wang F, Zhang D, Wan A, Rodrigues B. Endothelial cell regulation of cardiac metabolism following diabetes. *Cardiovasc Hematol Disord Drug Targets.* 2014; 14:121–125. [PubMed: 24801726]
3. Budzyn K, Marley PD, Sobey CG. Targeting rho and rho-kinase in the treatment of cardiovascular disease. *Trends Pharmacol Sci.* 2006; 27:97–104. [PubMed: 16376997]
4. Loirand G, Guerin P, Pacaud P. Rho kinases in cardiovascular physiology and pathophysiology. *Circ Res.* 2006; 98:322–334. [PubMed: 16484628]
5. Zhou H, Li YJ, Wang M, Zhang LH, Guo BY, Zhao ZS, et al. Involvement of rhoa/rock in myocardial fibrosis in a rat model of type 2 diabetes. *Acta Pharmacol Sin.* 2011; 32:999–1008. [PubMed: 21743486]
6. Chun CZ, Kaur S, Samant GV, Wang L, Pramanik K, Garnaas MK, et al. Snrk-1 is involved in multiple steps of angioblast development and acts via notch signaling pathway in artery-vein specification in vertebrates. *Blood.* 2009; 113:1192–1199. [PubMed: 18723694]
7. Cossette SM, Gastonguay AJ, Bao X, Lerch-Gaggl A, Zhong L, Harmann LM, et al. Sucrose non-fermenting related kinase enzyme is essential for cardiac metabolism. *Biol open.* 2014; BIO20149811.
8. Breckenridge RA, Piotrowska I, Ng KE, Ragan TJ, West JA, Kotecha S, et al. Hypoxic regulation of hand1 controls the fetal-neonatal switch in cardiac metabolism. *PLoS Biol.* 2013; 11:e1001666. [PubMed: 24086110]
9. Lopaschuk GD, Jaswal JS. Energy metabolic phenotype of the cardiomyocyte during development, differentiation, and postnatal maturation. *J Cardiovasc Pharmacol.* 2010; 56:130–140. [PubMed: 20505524]
10. Bhute VJ, Palecek SP. Metabolic responses induced by DNA damage and poly (adp-ribose) polymerase (parp) inhibition in mcf-7 cells. *Metabolomics.* 2015; 11:1779–1791. [PubMed: 26478723]
11. Weljie AM, Newton J, Mercier P, Carlson E, Slupsky CM. Targeted profiling: Quantitative analysis of 1h nmr metabolomics data. *Anal Chem.* 2006; 78:4430–4442. [PubMed: 16808451]

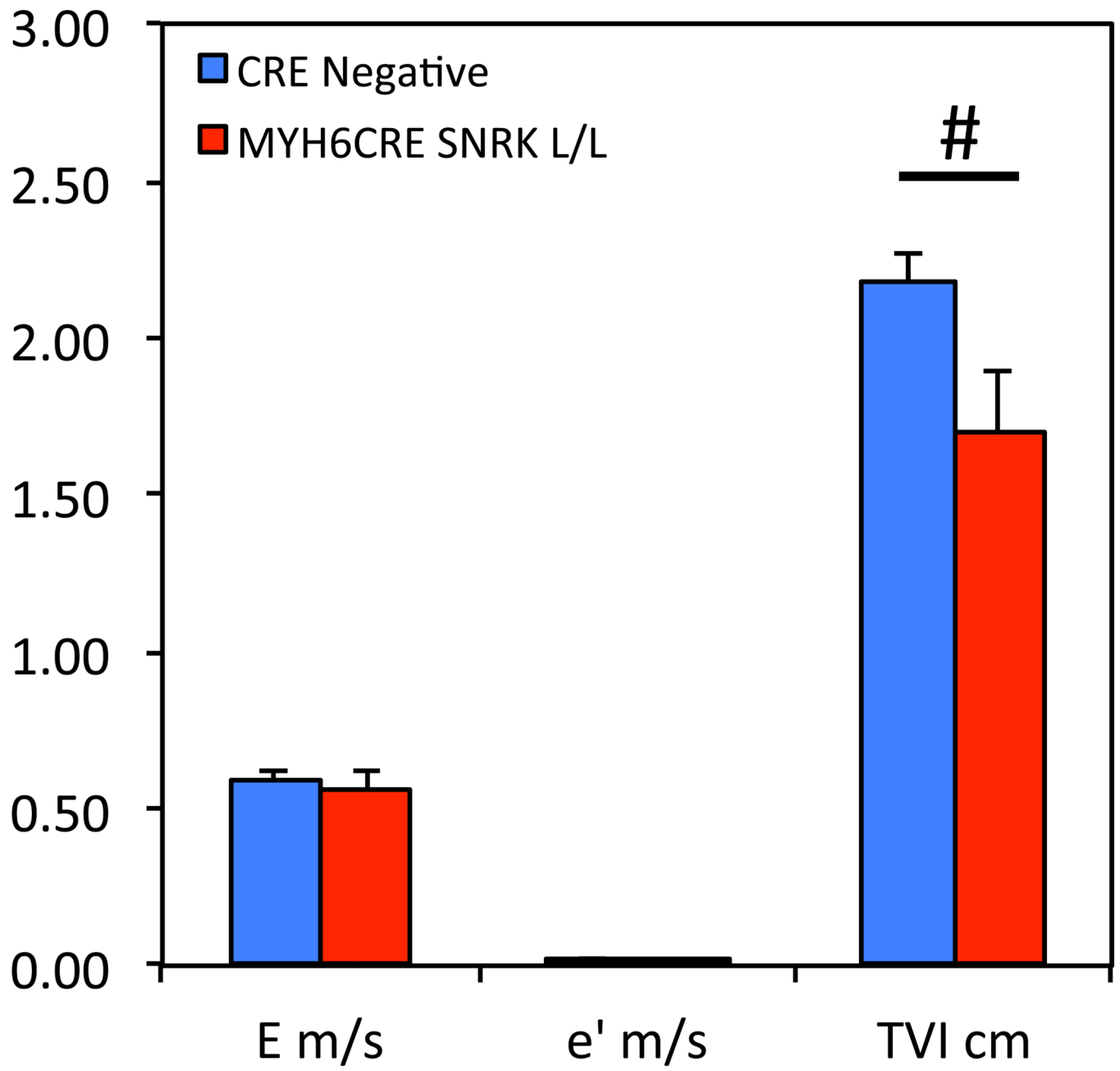
12. Wishart DS, Jewison T, Guo AC, Wilson M, Knox C, Liu Y, et al. Hmdb 3.0--the human metabolome database in 2013. *Nucleic Acids Res.* 2013; 41:D801–D807. [PubMed: 23161693]
13. Xia J, Sinelnikov IV, Han B, Wishart DS. Metaboanalyst 3.0--making metabolomics more meaningful. *Nucleic Acids Res.* 2015; 43:W251–W257. [PubMed: 25897128]
14. Agah R, Frenkel PA, French BA, Michael LH, Overbeek PA, Schneider MD. Gene recombination in postmitotic cells. Targeted expression of cre recombinase provokes cardiac-restricted, site-specific rearrangement in adult ventricular muscle in vivo. *J Clin Invest.* 1997; 100:169–179. [PubMed: 9202069]
15. Kim S, Iwao H. Molecular and cellular mechanisms of angiotensin ii-mediated cardiovascular and renal diseases. *Pharmacol Rev.* 2000; 52:11–34. [PubMed: 10699153]
16. Hibuse T, Maeda N, Nakatsuji H, Tochino Y, Fujita K, Kihara S, et al. The heart requires glycerol as an energy substrate through aquaporin 7, a glycerol facilitator. *Cardiovasc Res.* 2009; 83:34–41. [PubMed: 19297367]
17. Narayan M, Mirza SP, Twining SS. Identification of phosphorylation sites on extracellular corneal epithelial cell maspin. *Proteomics.* 2011; 11:1382–1390. [PubMed: 21365746]
18. Yang S, Kim HM. The rhoa-rock-pten pathway as a molecular switch for anchorage dependent cell behavior. *Biomaterials.* 2012; 33:2902–2915. [PubMed: 22244698]
19. Chang J, Xie M, Shah VR, Schneider MD, Entman ML, Wei L, et al. Activation of rho-associated coiled-coil protein kinase 1 (rock-1) by caspase-3 cleavage plays an essential role in cardiac myocyte apoptosis. *Proc Natl Acad Sci U S A.* 2006; 103:14495–14500. [PubMed: 16983089]
20. Liu Y, Suzuki YJ, Day RM, Fanburg BL. Rho kinase-induced nuclear translocation of erk1/erk2 in smooth muscle cell mitogenesis caused by serotonin. *Circ Res.* 2004; 95:579–586. [PubMed: 15297378]
21. Kobayashi N, Horinaka S, Mita S, Nakano S, Honda T, Yoshida K, et al. Critical role of rho-kinase pathway for cardiac performance and remodeling in failing rat hearts. *Cardiovasc Res.* 2002; 55:757–767. [PubMed: 12176125]
22. Hattori T, Shimokawa H, Higashi M, Hiroki J, Mukai Y, Tsutsui H, et al. Long-term inhibition of rho-kinase suppresses left ventricular remodeling after myocardial infarction in mice. *Circulation.* 2004; 109:2234–2239. [PubMed: 15096457]
23. Shi J, Wei L. Rho kinases in cardiovascular physiology and pathophysiology: The effect of fasudil. *J Cardiovasc Pharmacol.* 2013; 62:341–354.
24. Becker W, Heukelbach J, Kentrup H, Joost HG. Molecular cloning and characterization of a novel mammalian protein kinase harboring a homology domain that defines a subfamily of serine/threonine kinases. *Eur J Biochem.* 1996; 235:736–743. [PubMed: 8654423]
25. Guttman M, Russell P, Ingolia NT, Weissman JS, Lander ES. Ribosome profiling provides evidence that large noncoding rnas do not encode proteins. *Cell.* 2013; 154:240–251. [PubMed: 23810193]
26. D'Souza K, Nzirorera C, Kienesberger PC. Lipid metabolism and signaling in cardiac lipotoxicity. *Biochim Biophys Acta.* 2016
27. Appuhamy JA, Nayananjalie WA, England EM, Gerrard DE, Akers RM, Hanigan MD. Effects of amp-activated protein kinase (ampk) signaling and essential amino acids on mammalian target of rapamycin (mTOR) signaling and protein synthesis rates in mammary cells. *J Dairy Sci.* 2014; 97:419–429. [PubMed: 24183687]
28. O'Neill HM, Holloway GP, Steinberg GR. Ampk regulation of fatty acid metabolism and mitochondrial biogenesis: Implications for obesity. *Mol Cell Endocrinol.* 2013; 366:135–151. [PubMed: 22750049]
29. Nagoshi T, Yoshimura M, Rosano GM, Lopaschuk GD, Mochizuki S. Optimization of cardiac metabolism in heart failure. *Curr Pharm Des.* 2011; 17:3846–3853. [PubMed: 21933140]
30. Stanley WC, Recchia FA, Lopaschuk GD. Myocardial substrate metabolism in the normal and failing heart. *Physiol Rev.* 2005; 85:1093–1129. [PubMed: 15987803]
31. Davila-Roman VG, Vedala G, Herrero P, de las Fuentes L, Rogers JG, Kelly DP, et al. Altered myocardial fatty acid and glucose metabolism in idiopathic dilated cardiomyopathy. *J Am Coll Cardiol.* 2002; 40:271–277. [PubMed: 12106931]

32. O'Donnell JM, Fields AD, Sorokina N, Lewandowski ED. The absence of endogenous lipid oxidation in early stage heart failure exposes limits in lipid storage and turnover. *J Mol Cell Cardiol.* 2008; 44:315–322. [PubMed: 18155232]
33. Boudina S, Sena S, O'Neill BT, Tathireddy P, Young ME, Abel ED. Reduced mitochondrial oxidative capacity and increased mitochondrial uncoupling impair myocardial energetics in obesity. *Circulation.* 2005; 112:2686–2695. [PubMed: 16246967]
34. Wang GG, Li W, Lu XH, Zhao X, Xu L. Taurine attenuates oxidative stress and alleviates cardiac failure in type i diabetic rats. *Croat Med J.* 2013; 54:171–179. [PubMed: 23630144]
35. Schaffer SW, Jong CJ, Ramila KC, Azuma J. Physiological roles of taurine in heart and muscle. *J Biomed Sci.* 2010; 17(Suppl 1):S2. [PubMed: 20804594]
36. Rikitake Y, Oyama N, Wang CY, Noma K, Satoh M, Kim HH, et al. Decreased perivascular fibrosis but not cardiac hypertrophy in rock1+/- haploinsufficient mice. *Circulation.* 2005; 112:2959–2965. [PubMed: 16260635]
37. Wang S, Sun A, Li L, Zhao G, Jia J, Wang K, et al. Up-regulation of bmp-2 antagonizes tgfbeta1/rock-enhanced cardiac fibrotic signalling through activation of smurf1/smad6 complex. *J Cell Mol Med.* 2012; 16:2301–2310. [PubMed: 22283839]
38. Sakabe M, Sakata H, Matsui H, Ikeda K, Yamagishi T, Nakajima Y. Rock1 expression is regulated by tgfbeta3 and alk2 during valvuloseptal endocardial cushion formation. *Anat Rec.* 2008; 291:845–857.
39. Soga J, Noma K, Hata T, Hidaka T, Fujii Y, Idei N, et al. Rho-associated kinase activity, endothelial function, and cardiovascular risk factors. *Arterioscler Thromb Vasc Biol.* 2011; 31:2353–2359. [PubMed: 21737782]
40. Zhao Z, Rivkees SA. Rho-associated kinases play a role in endocardial cell differentiation and migration. *Dev Biol.* 2004; 275:183–191. [PubMed: 15464581]
41. Shi J, Zhang YW, Yang Y, Zhang L, Wei L. Rock1 plays an essential role in the transition from cardiac hypertrophy to failure in mice. *J Mol Cell Cardiol.* 2010; 49:819–828. [PubMed: 20709073]
42. Rines AM, Wu R, Khechaduri A, Burke MA, Sato T, Abdelwahid E, et al. Abstract: Snf1-related kinase improves cardiac metabolic efficiency through a decrease in mitochondrial uncoupling. *Circulation.* 2014:A14048.
43. Rines A, Burke MA, Wu R, Abel DA, Ardehali H. Abstract: Transgenic overexpression of snf1-related kinase in the heart improves cardiac metabolic efficiency and response to myocardial ischemia. *Circ Res.* 2012:A11.

Clinical Perspective

Dilated cardiomyopathy (DCM) is a disorder where the heart becomes enlarged, and its function is compromised. DCM is influenced by several factors, and recent evidence point to alteration in cardiac metabolism especially in conjunction with diabetes as a possible factor. Previously, our laboratory has identified a serine threonine kinase in the adenosine monophosphate activated protein kinase (AMPK) family namely sucrose non-fermenting related kinase (SNRK) that plays a critical role in cardiac metabolism in mammals. Others have implicated SNRK as a suppressor of adipocyte inflammation. In this study, we investigated the hypothesis that SNRK-induced signal transduction in cardiomyocytes is critical for maintaining its cardiac function in mammals. Using echocardiography on *Snrk* cardiac conditional knockout mice, we show here that these mice have cardiac function deficits that resemble DCM phenotype, and these deficits are in part due to major changes in the metabolites involved in fatty acid oxidation in cardiomyocytes. We then identified using phosphopeptide-based proteomic screen, Rho-Associated Kinase1 (ROCK1) that serves as a putative substrate for SNRK in cardiomyocytes. ROCK1 is a kinase that is involved in regulating muscle contraction, and has been previously implicated in several cardiovascular diseases such as atherosclerosis, cardiac hypertrophy and diabetes. Importantly, elevated ROCK activity and endothelial dysfunction was associated as chief risk factors that lead to the progression of cardiovascular disease and outcome in the Framingham heart study. This study therefore provides the molecular link associated with the elevated ROCK activity in cardiomyocytes of the mammalian heart, and delineates SNRK as a target for DCM. Biochemical analysis in vivo confirmed that *Snrk* cardiac conditional mice showed elevated ROCK activity, which was rescued partially by ROCK inhibitor Fasudil. Importantly, the Fasudil rescue restored some of the cardiac functional parameters in *Snrk* cardiac conditional knockout mice thus implying SNRK-ROCK signaling pathway as a critical pathway in cardiomyocyte that mediates cardiac function, and elevates this interface for drug discovery in cardiovascular disease.

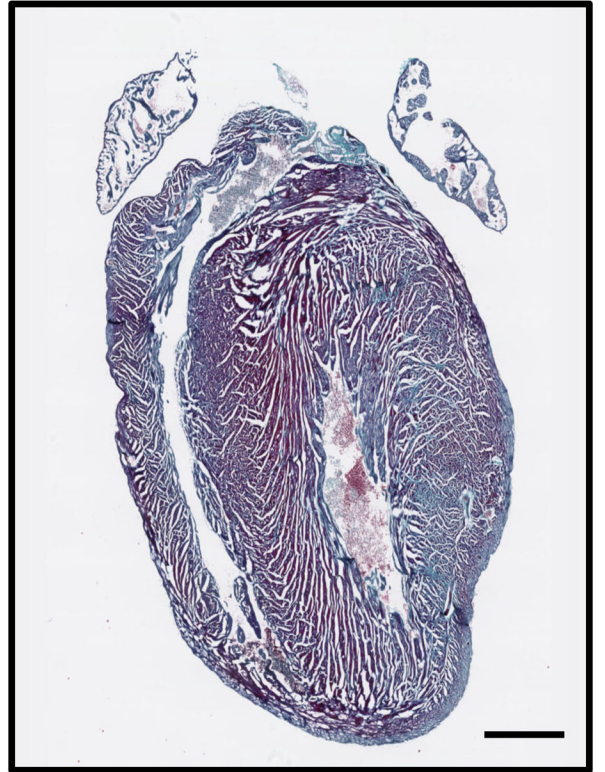




CRE negative

MYH6CRE SNRK L/L

Cardiomyocyte



Quantification of Trichrome Staining

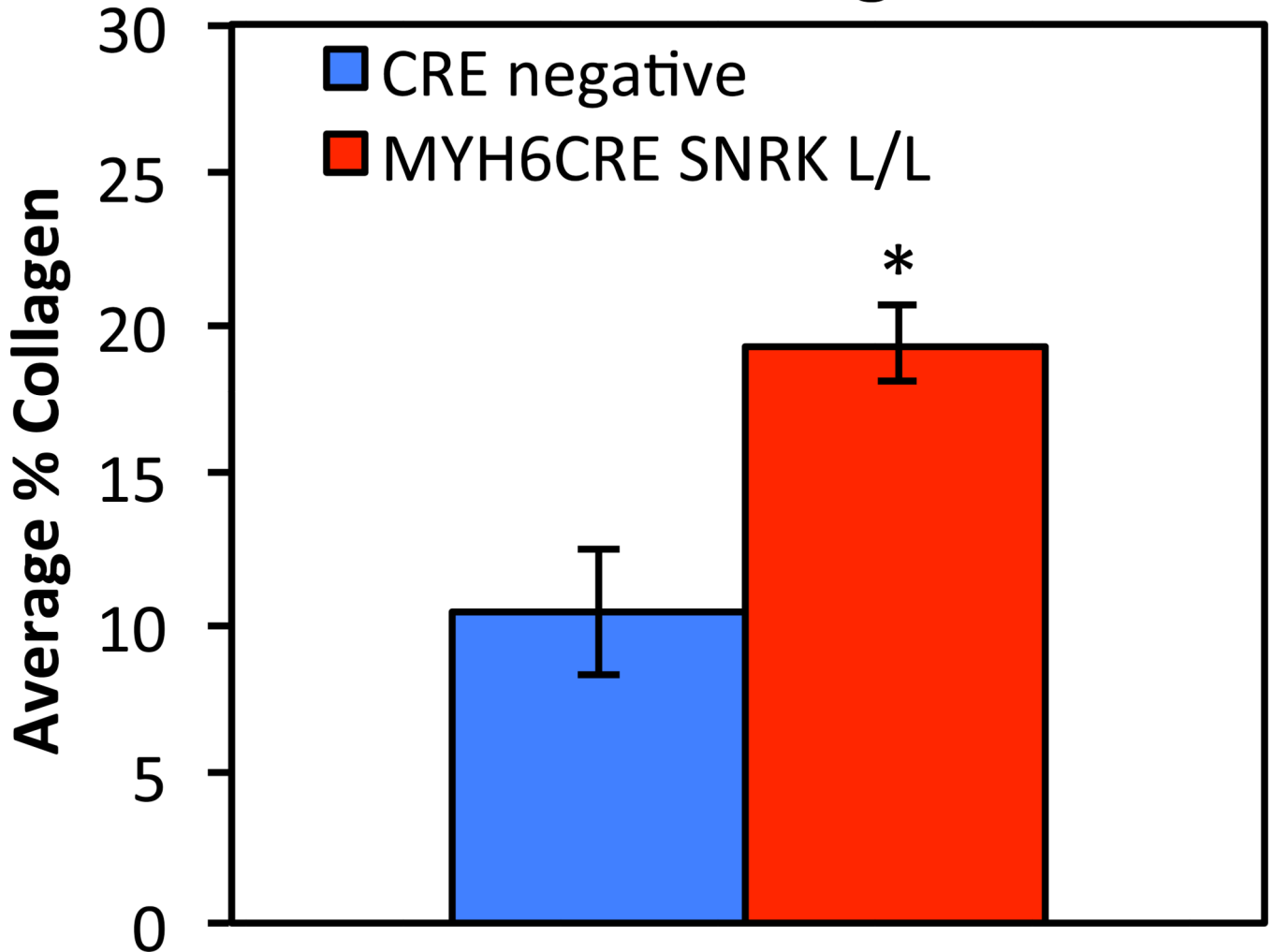


Figure 1.

Cardiomyocyte-conditional SNRK null mice (*Snrk* cmcKO) ECHO results. ECHO was performed on 6 month adult *Snrk* WT and cmcKO males as described in the materials and methods. Panel A describes strain and strain rate imaging analyses by ECHO. Panel B indicates isovolumic relaxation time (IVRT) msec, a parameter for diastolic function, ratio of mitral peak velocity of early filling (E) m to early diastolic mitral annular velocity (e') (E/e' ratio), pulmonary acceleration time (PAT) msec, ejection time (ET) msec and ratio of PAT to ET. Panel C shows time-velocity integrals (TVI) cm along with mitral peak velocity (E) m/s and diastolic mitral annular velocity (e') m/s. Panel D are representative images of Gomori's Trichrome staining in CRE negative or cardiomyocyte specific conditional null (MYH6CRE SNRK L/L) adult mouse hearts. Panel E, shows average percent collagen

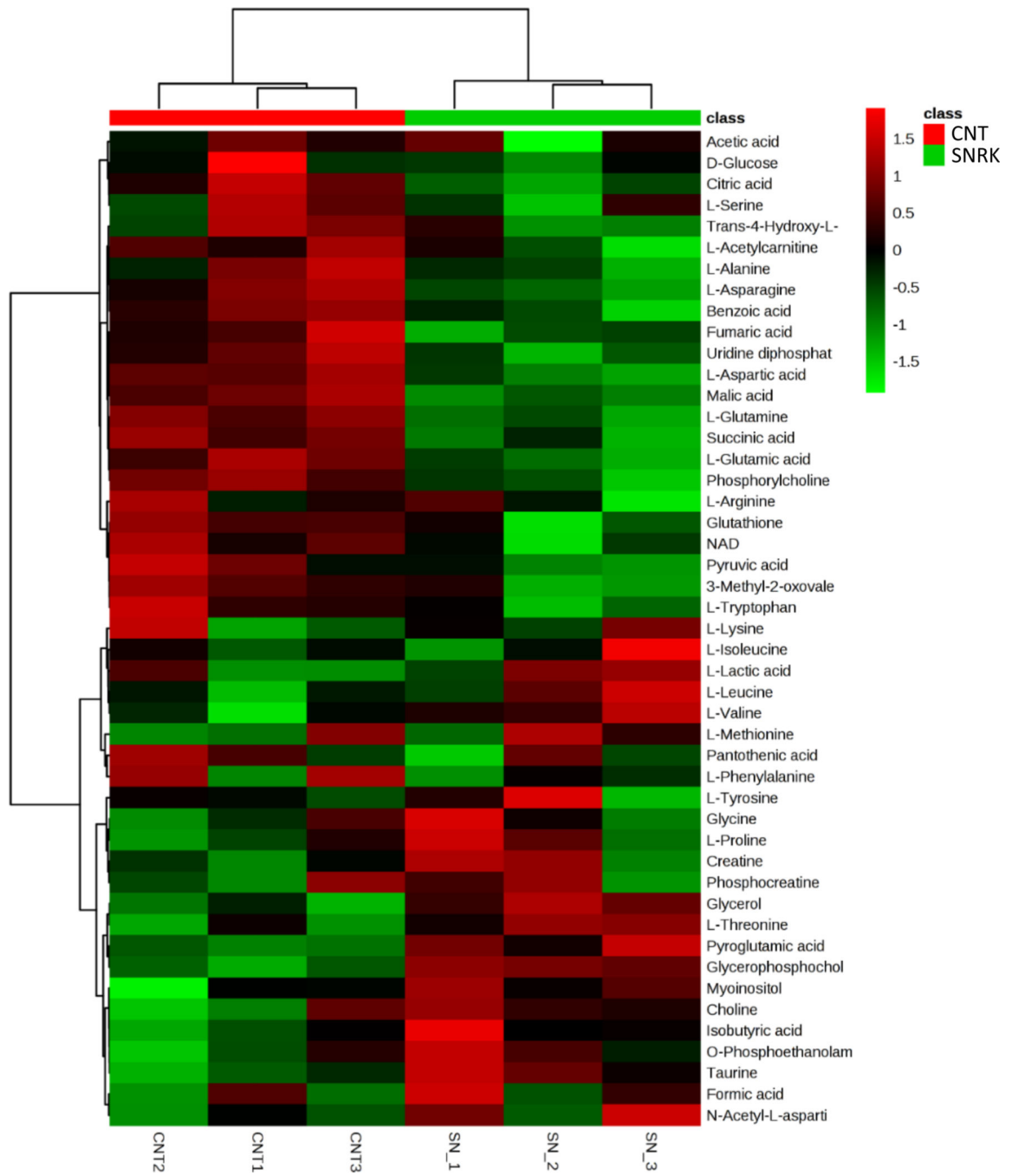
staining in CRE negative MYH6CRE SNRK L/L adult mouse hearts. The number of mice per group equals 3–5. *= $p < 0.05$, #= $p < 0.1$. Scale bar = 1mm

Author Manuscript

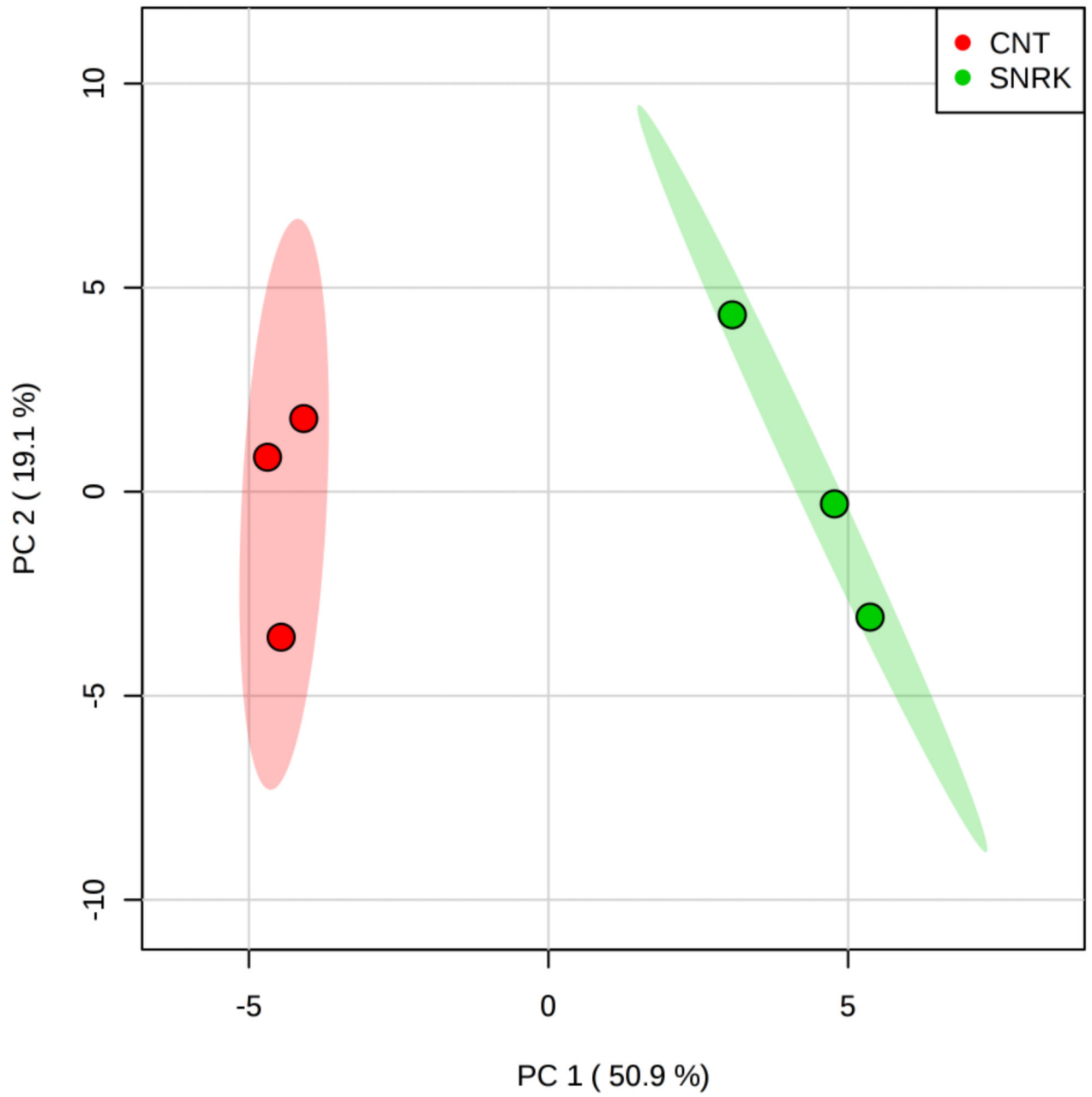
Author Manuscript

Author Manuscript

Author Manuscript



Scores Plot



| PATHWAY | Hits | Raw p | FDR | Impact |
|---|------|----------|----------|---------|
| Citrate cycle (TCA cycle) | 4 | 3.47E-06 | 0.000181 | 0.1875 |
| Arginine and proline metabolism | 10 | 0.000141 | 0.00359 | 0.26214 |
| Nitrogen metabolism | 10 | 0.000212 | 0.00359 | 0.26922 |
| Tyrosine metabolism | 4 | 0.000287 | 0.00359 | 0.07778 |
| Butanoate metabolism | 4 | 0.000345 | 0.00359 | 0.08 |
| Glyoxylate and dicarboxylate metabolism | 4 | 0.000985 | 0.007407 | 0.09091 |
| Glutathione metabolism | 4 | 0.000997 | 0.007407 | 0.17742 |
| D-Glutamine and D-glutamate metabolism | 2 | 0.001398 | 0.008076 | 0.33334 |
| Nicotinate and nicotinamide metabolism | 4 | 0.001857 | 0.009467 | 0.07273 |
| Porphyrin and chlorophyll metabolism | 3 | 0.002063 | 0.009467 | 0.02631 |
| Pyrimidine metabolism | 1 | 0.002441 | 0.009467 | 0.01031 |
| Alanine, aspartate and glutamate metabolism | 9 | 0.002597 | 0.009467 | 0.68571 |
| Phenylalanine metabolism | 6 | 0.002745 | 0.009467 | 0.16363 |
| Taurine and hypotaurine metabolism | 4 | 0.002913 | 0.009467 | 0.43479 |
| Histidine metabolism | 2 | 0.003549 | 0.010856 | 0.02 |
| beta-Alanine metabolism | 2 | 0.006719 | 0.019411 | 0.0303 |
| Aminoacyl-tRNA biosynthesis | 18 | 0.00907 | 0.024467 | 0.35486 |
| Cyanoamino acid metabolism | 4 | 0.00941 | 0.024467 | 0.24999 |
| Glycine, serine and threonine metabolism | 8 | 0.010867 | 0.026908 | 0.38983 |
| Pantothenate and CoA biosynthesis | 4 | 0.012511 | 0.029572 | 0.15151 |
| Purine metabolism | 2 | 0.015158 | 0.033194 | 0.00714 |
| Glycerophospholipid metabolism | 4 | 0.01532 | 0.033194 | 0.1233 |
| Cysteine and methionine metabolism | 6 | 0.016594 | 0.033931 | 0.09878 |
| Glycerolipid metabolism | 1 | 0.016965 | 0.033931 | 0.11111 |
| Propanoate metabolism | 3 | 0.026944 | 0.051893 | 0.06249 |
| Amino sugar and nucleotide sugar metabolism | 2 | 0.044392 | 0.082443 | 0.06422 |
| Lysine biosynthesis | 2 | 0.047813 | 0.085734 | 0.05714 |

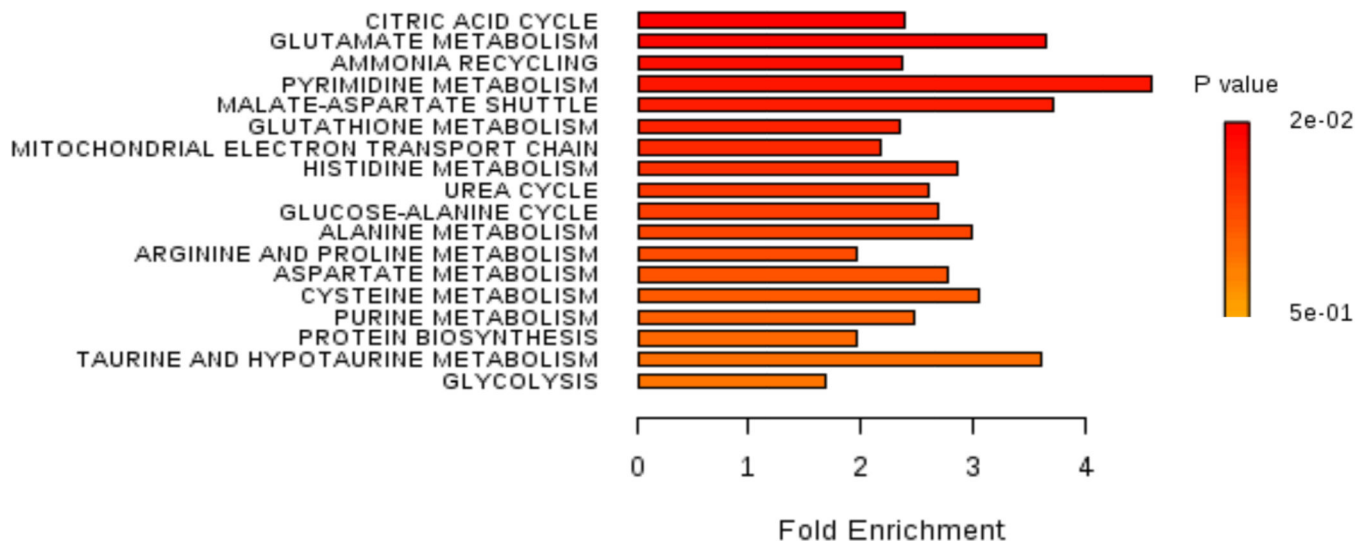


Figure 2.

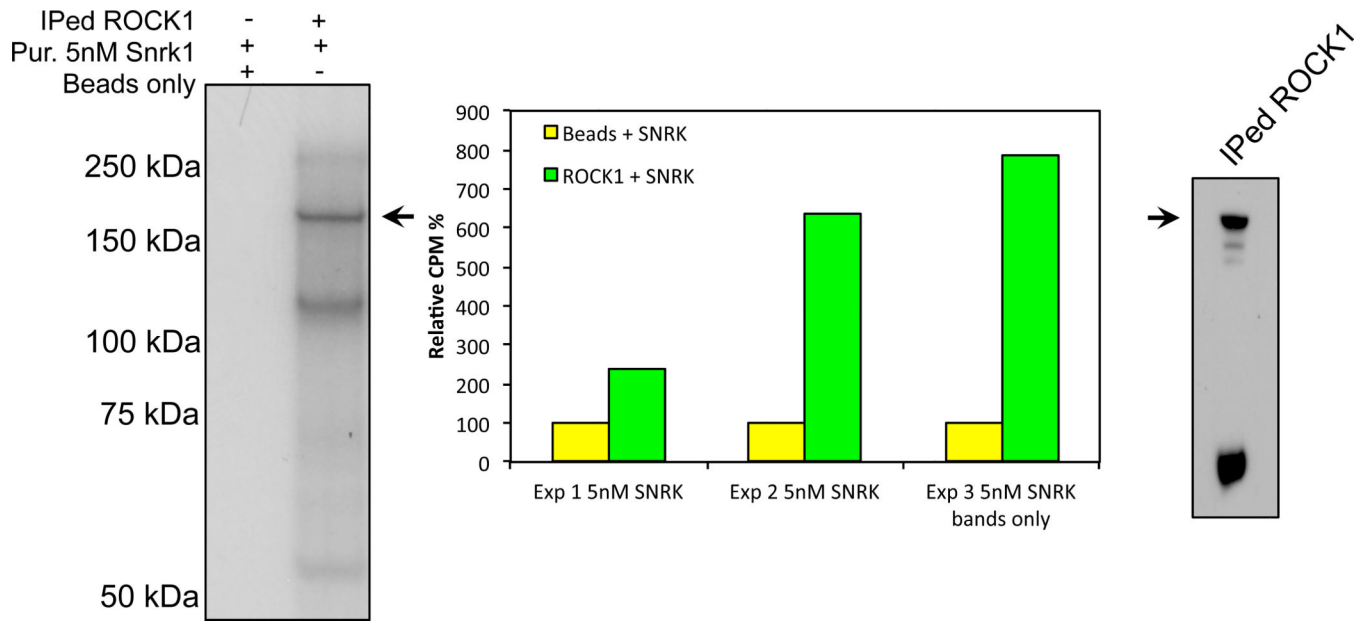
Loss of SNRK results in altered metabolomic profiles. Panel A. Heat map depicting the altered identified metabolites in non-silencing shRNA control (CNT) and shSNRK knockdown (SNRK) cardiomyocytes. Panel B Score Plot analysis for principle components (PC) between the non-silencing shRNA control (CNT) red and shSNRK knockdown (SNRK) green cardiomyocytes. Panel C Pathway topology analysis. Panel D. Metabolite set enrichment analysis was used to identify significantly enriched pathways ($p < 0.05$).

Author Manuscript

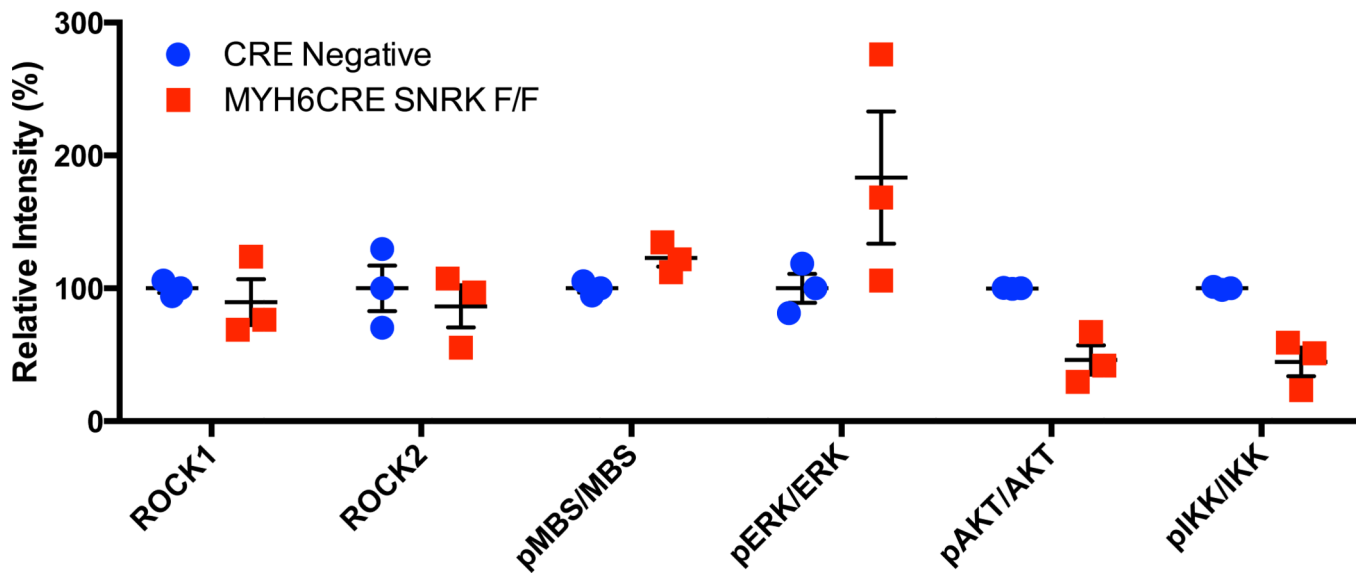
Author Manuscript

Author Manuscript

Author Manuscript



MYH6CRE Adult Heart Analysis



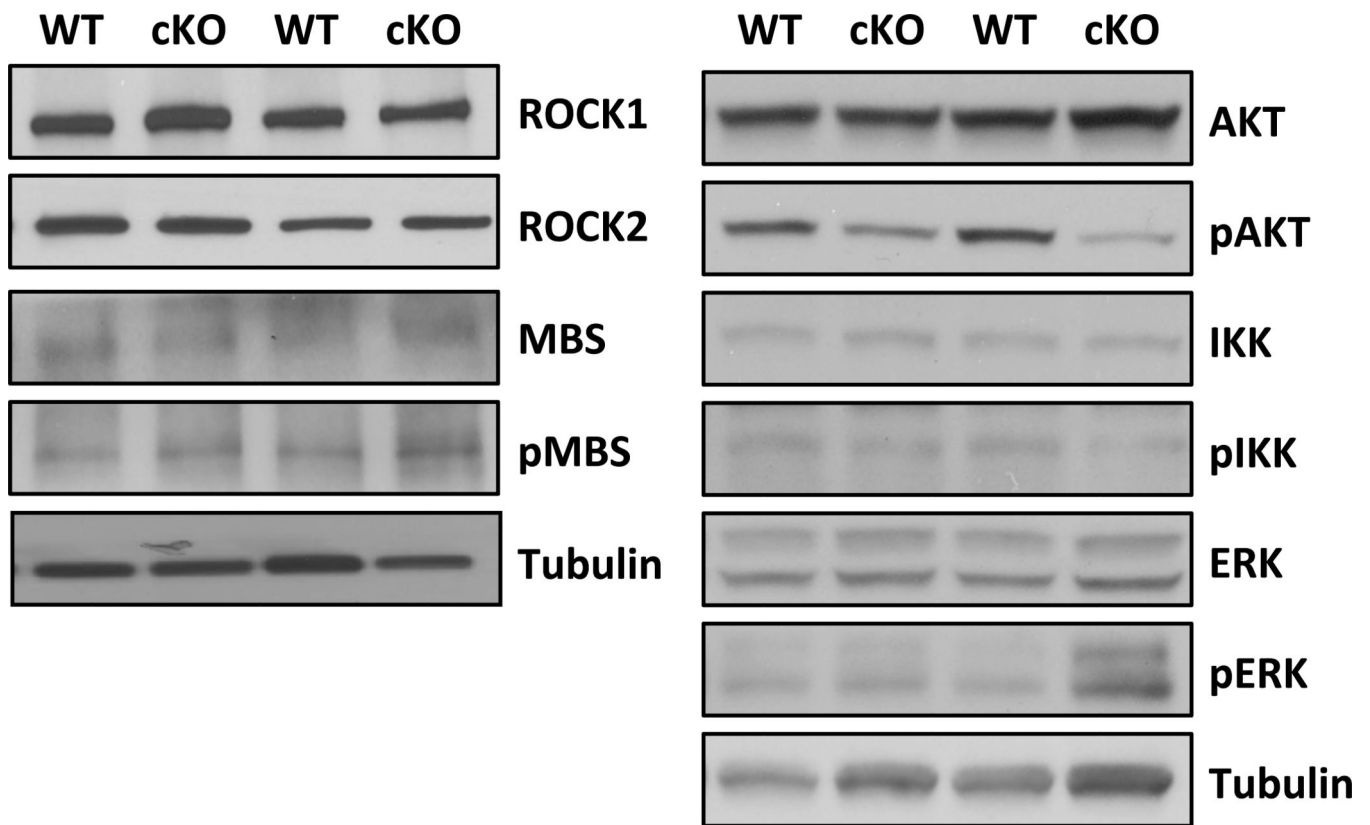
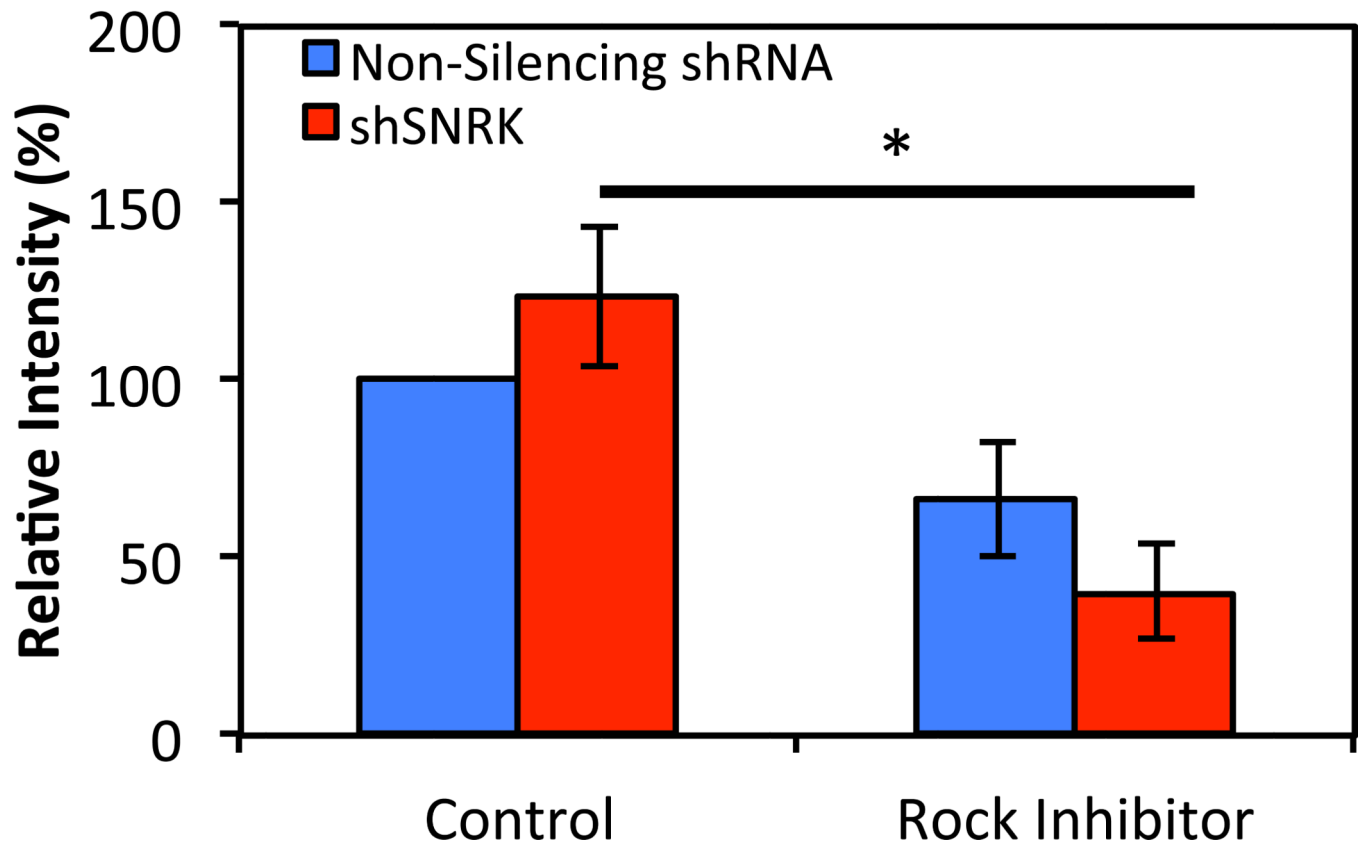
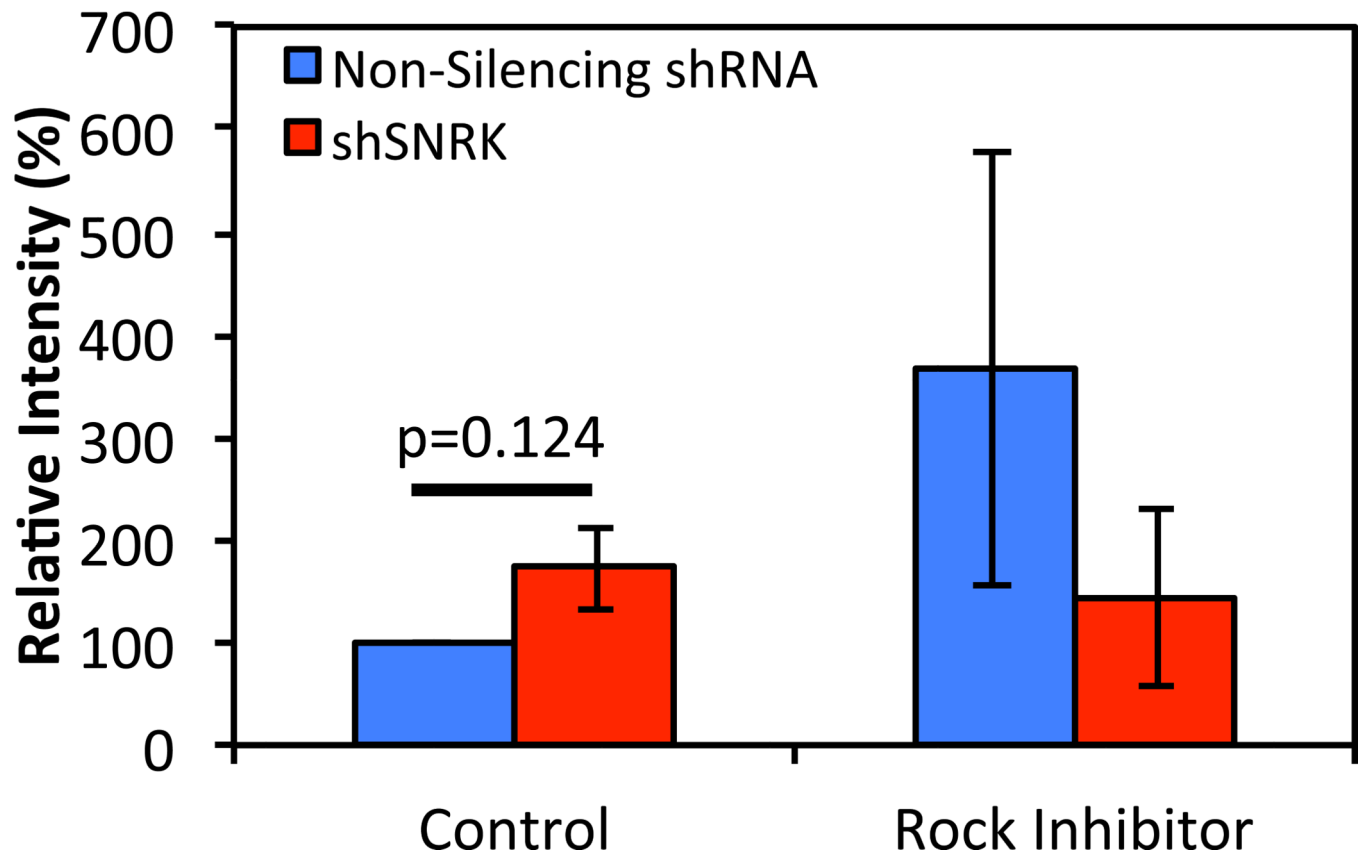


Figure 3. SNRK phosphorylation of ROCK, and influences on its activity in *Snrk* cmcKO adult hearts. Panel A shows direct phosphorylation of immunoprecipitated ROCK1 from human umbilical vein endothelial cells. Quantitation of the radioactive band in A is shown, and the successful immunoprecipitation of ROCK1 is demonstrated with the ROCK antibody on IPed lysates. Arrow denotes ROCK1 band. Data represents 3–4 independent experiments. Panel B western blot quantitation on lysates from cardiomyocyte-deleted SNRK adult hearts. Panel C representative western blot images from 4 independent heart lysates. The number of mice per group equals 3.

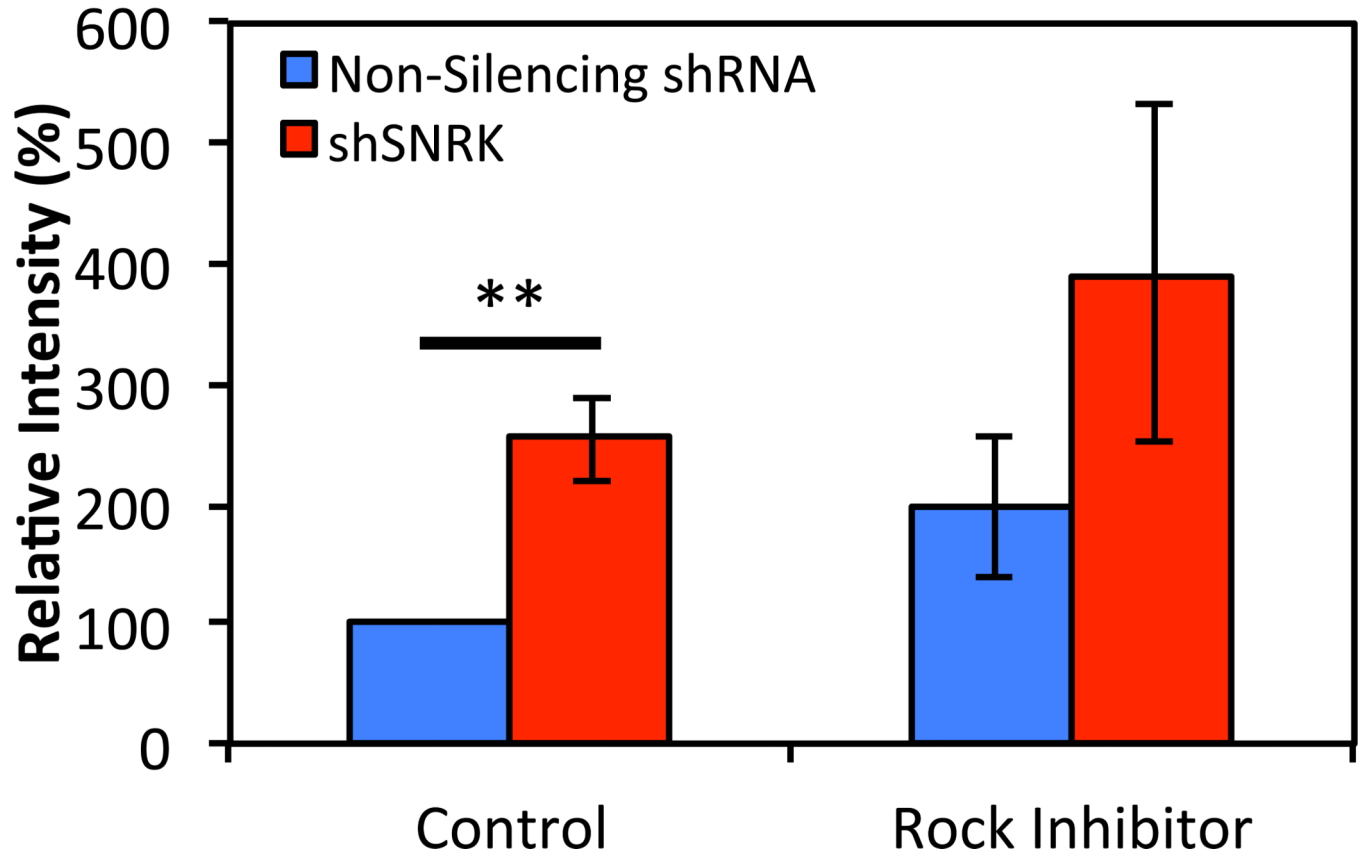
Cardiomyocyte pMBS/MBS Ratio



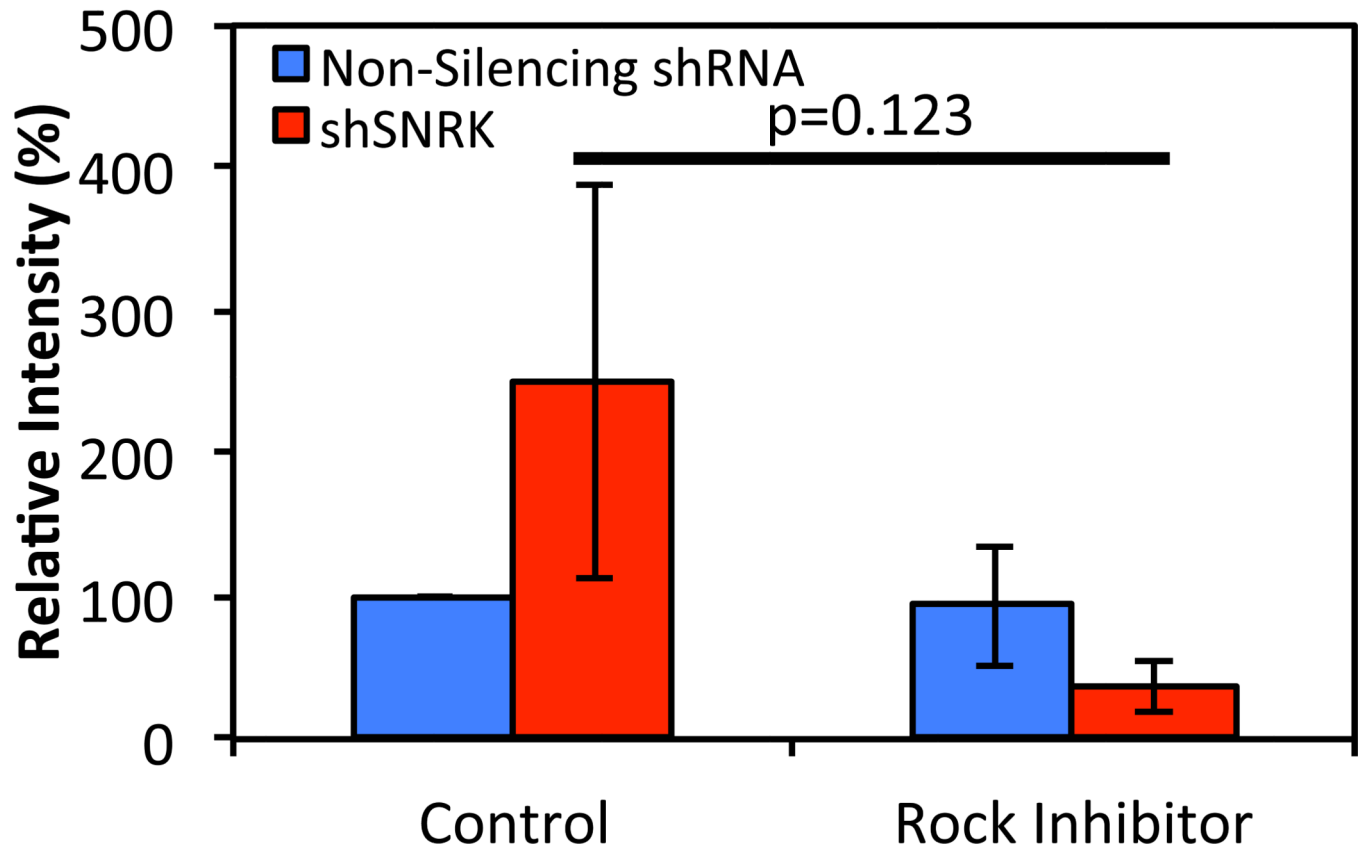
Cardiomyocyte pAKT/AKT Ratio



Cardiomyocyte pIKK/IKK Ratio



Cardiomyocyte pERK/ERK Ratio



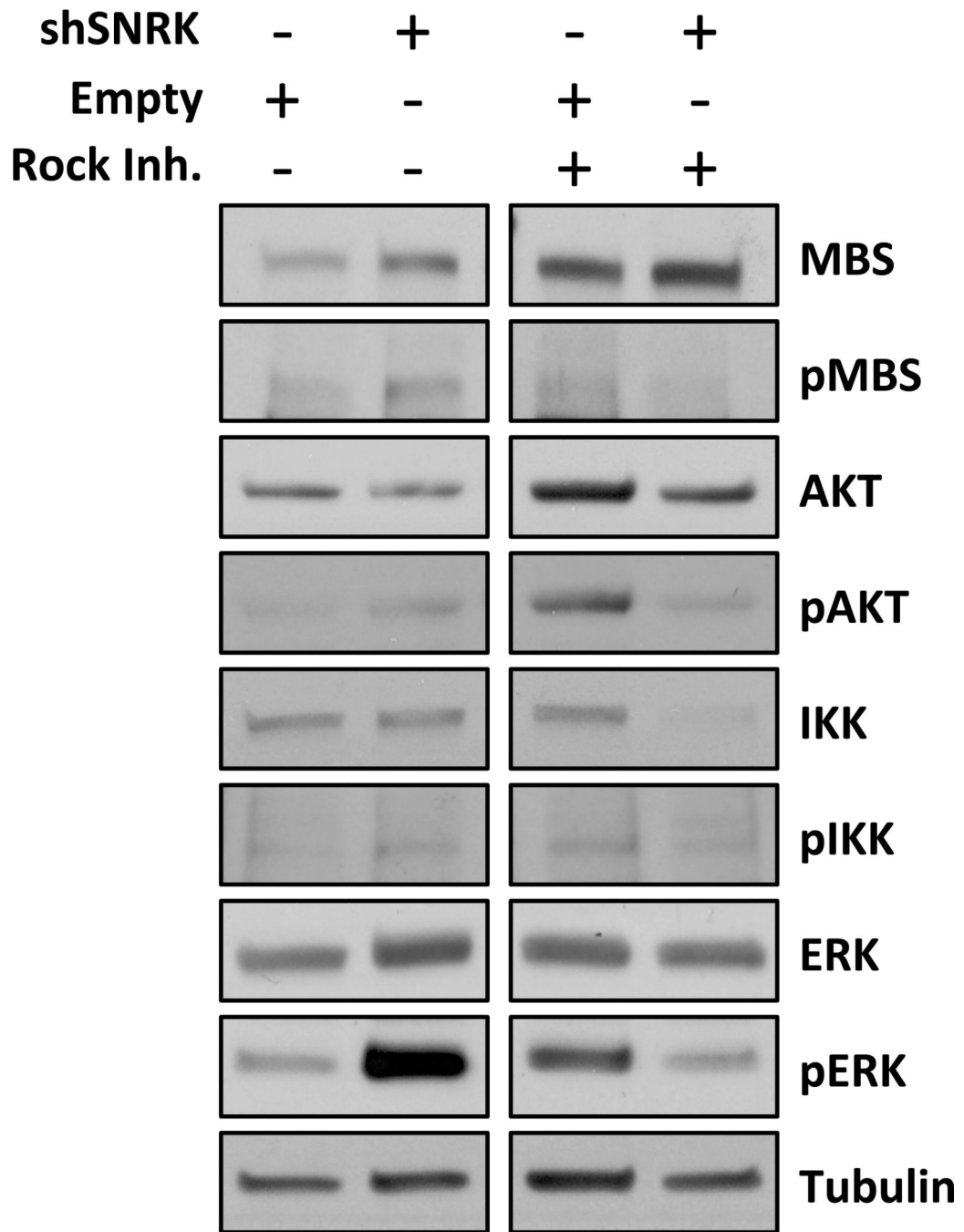
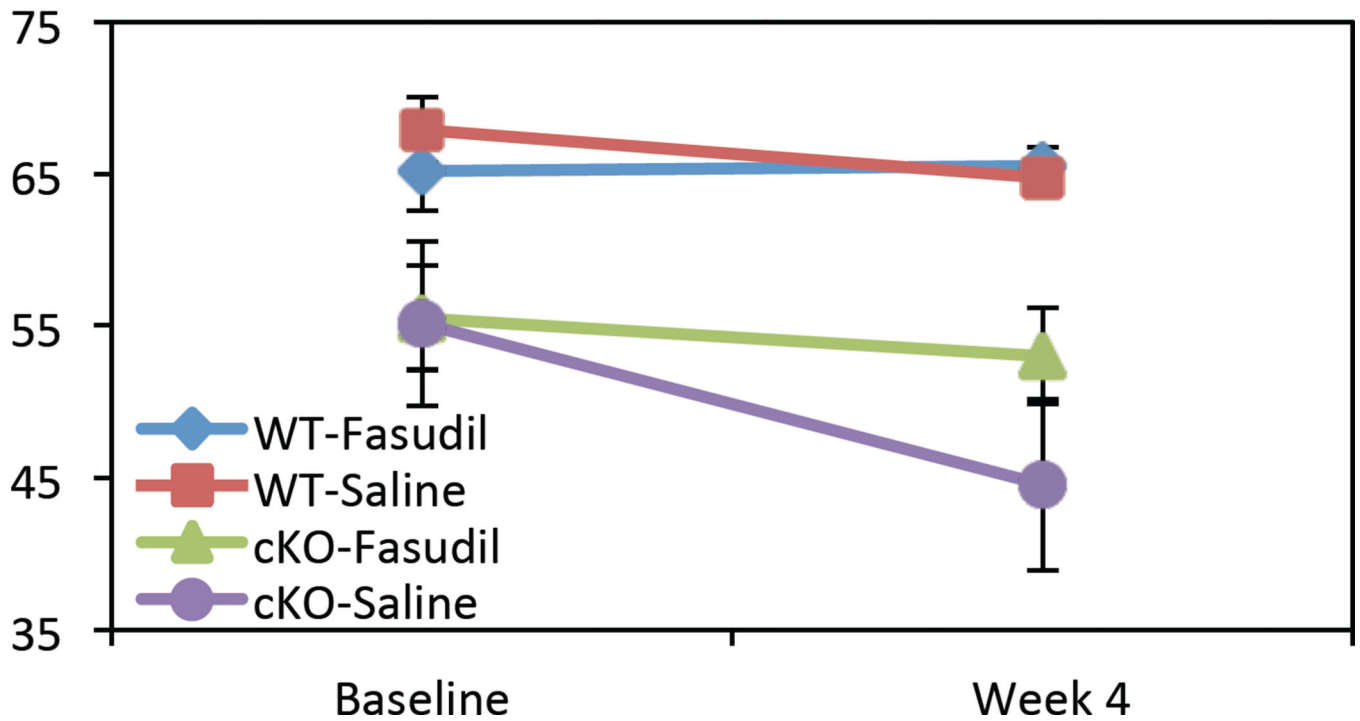
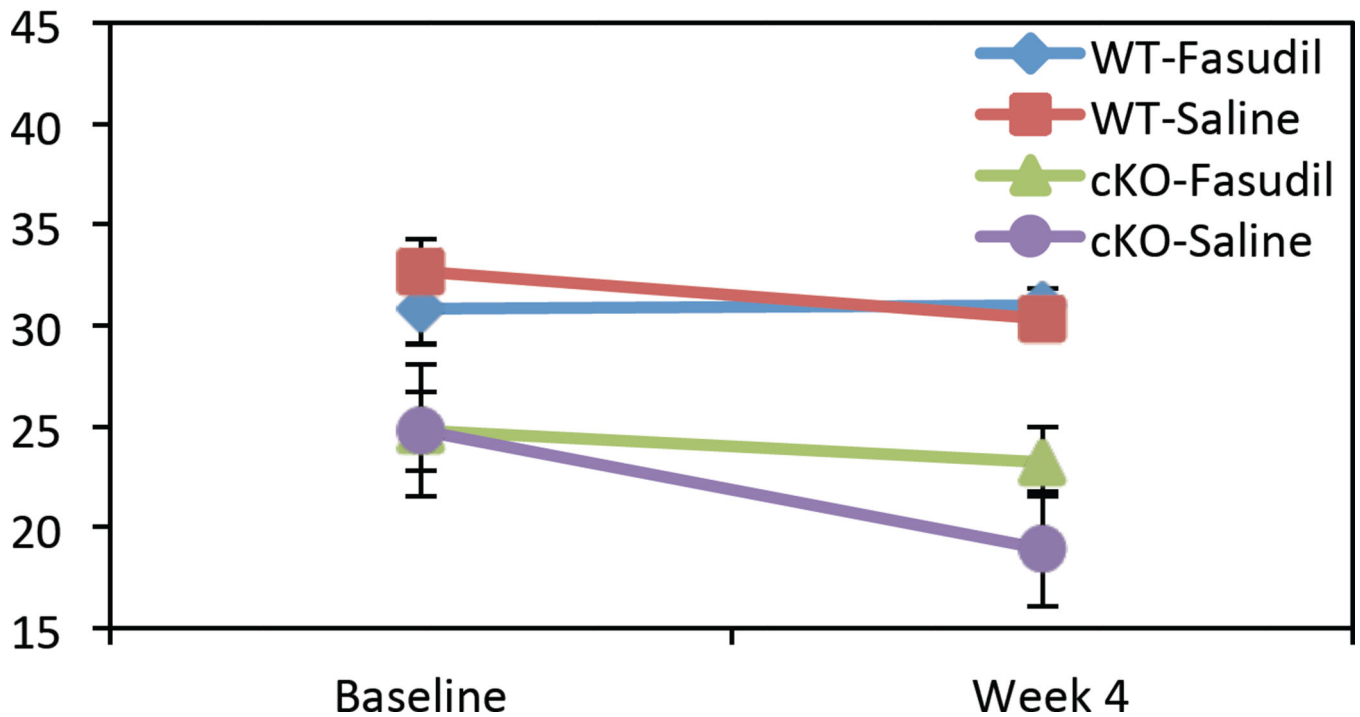


Figure 4. Loss of *Snrk* in cardiomyocytes results in increased ROCK activity. Western blots were performed on cardiomyocytes as described in materials and methods. Panel A-D western blot quantification of cardiomyocytes treated with water (Control), or 5 uM ROCK Inhibitor Y27632. Data represents 3–4 independent experiments. *= $p < 0.05$, **= $p < 0.0125$.

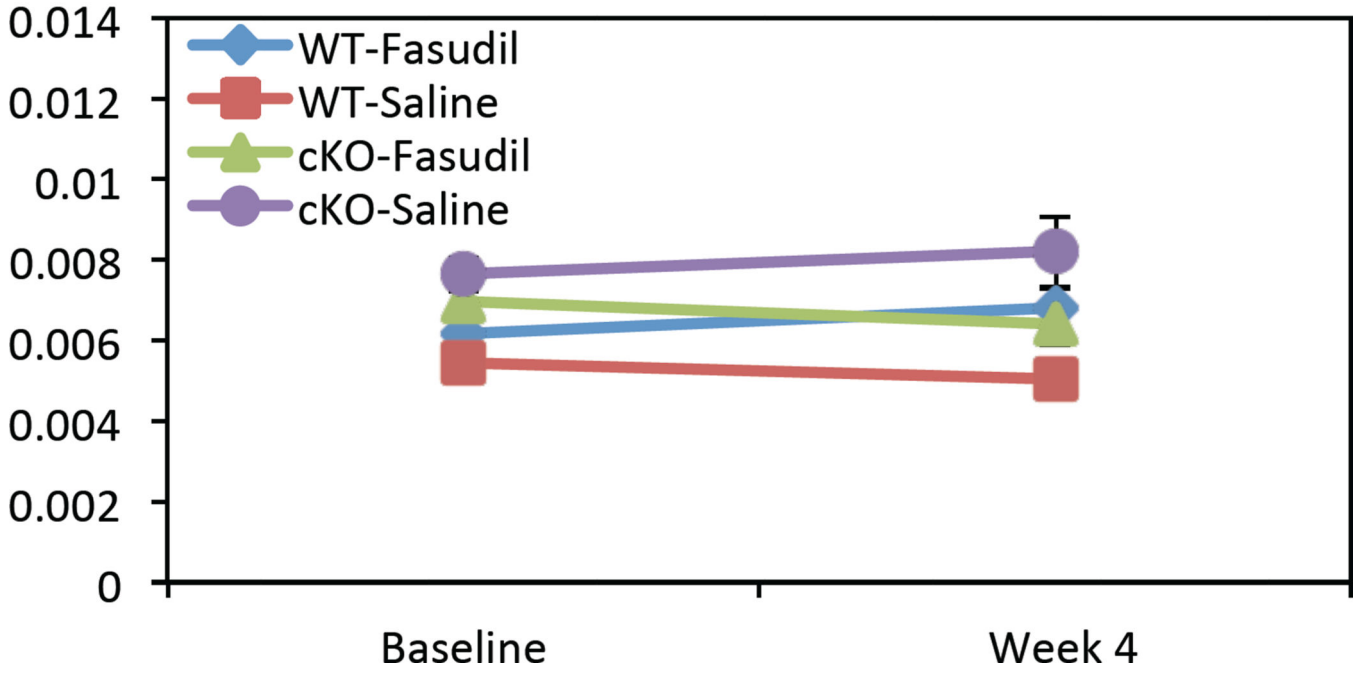
Ejection Fraction (EF) %



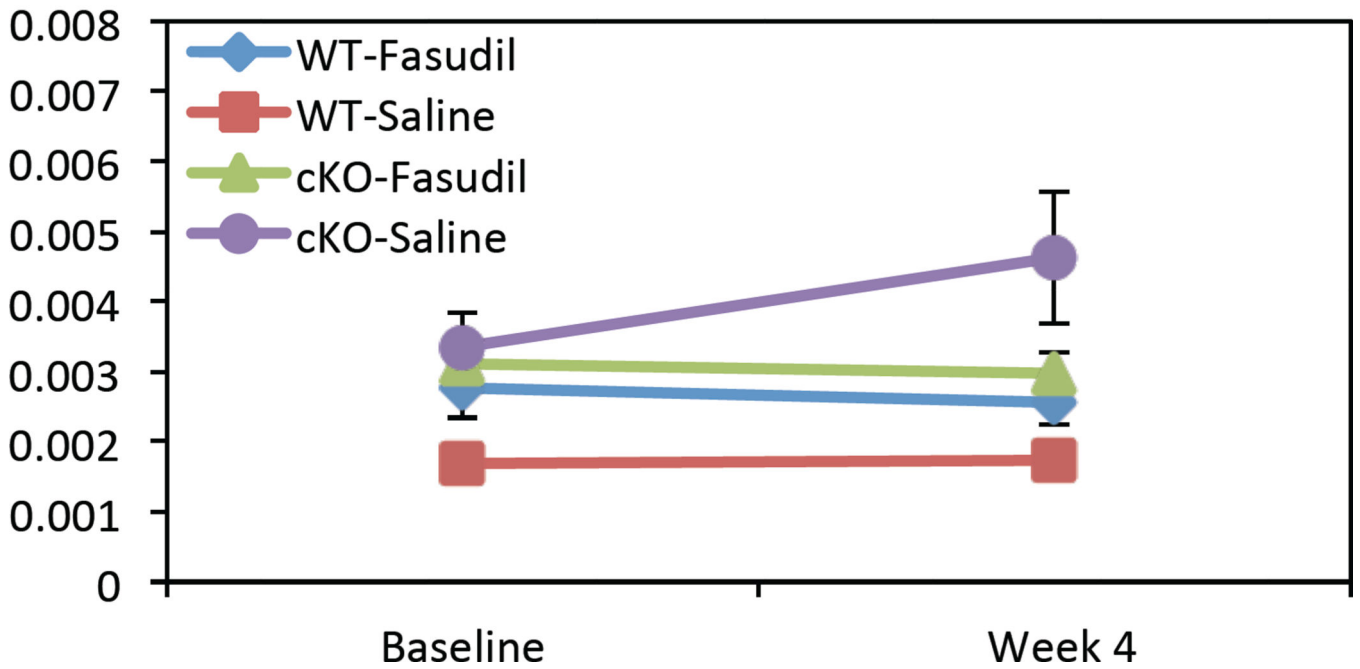
Fractional Shortening (FS) %



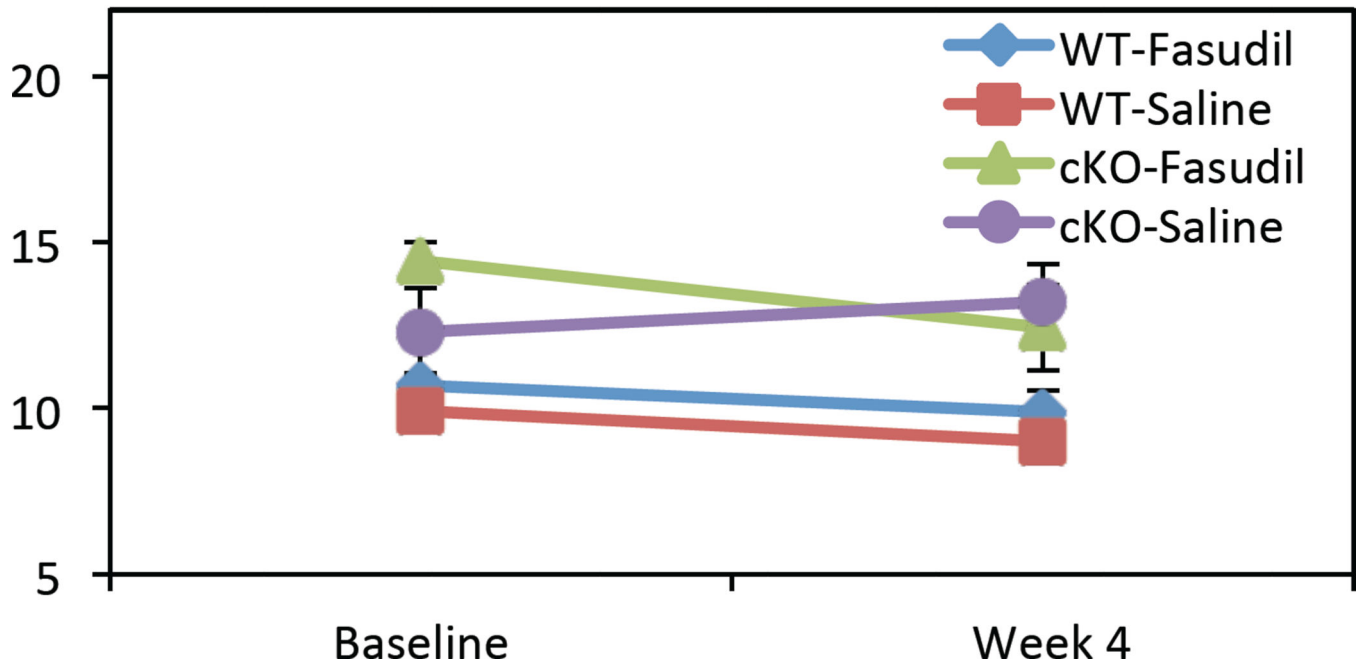
End Diastolic Volume/BW (ml/g)



End Systolic Volume/BW (ml/g)



Isovolumic relaxation time (IVRT) msec



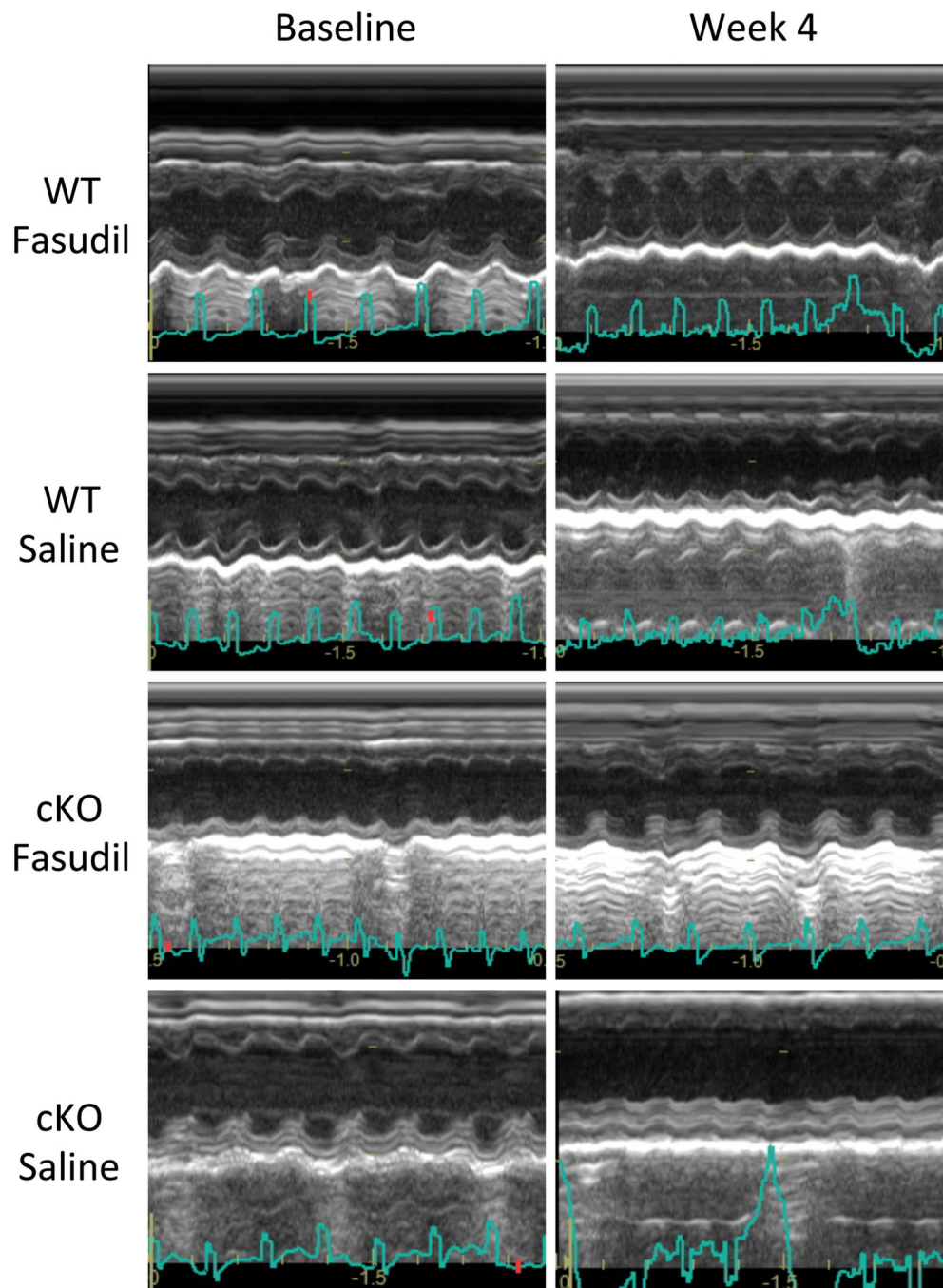


Figure 5. Inhibition of ROCK signaling improved cardiac function in cardiomyocyte-conditional SNRK null mice (*Snrk* cmcKO). ECHO was performed on 6–4 month adult male and female *Snrk* WT and *Snrk* cmcKO mice immediately prior to treatment and after 4 weeks. The mice received daily injections of saline or fasudil as described in the materials and methods. Panel A and B describes left ventricular (LV) function parameters EF % and FS %. Panel C and D describes the EDV and ESV which were normalized to body weight (BW). Panel E indicates the IVRT msec. Panel F is a representative M-Mode images from the mouse hearts at

baseline or after 4 weeks of daily fasudil or saline injections. There were 2 males and 2 females in the saline treated *Snrk* cmcKO and *Snrk* WT groups and 2 males and 3 females in the fasudil treated *Snrk* cmcKO and *Snrk* WT groups. See Table S5 for complete data set.

Author Manuscript

Author Manuscript

Author Manuscript

Author Manuscript

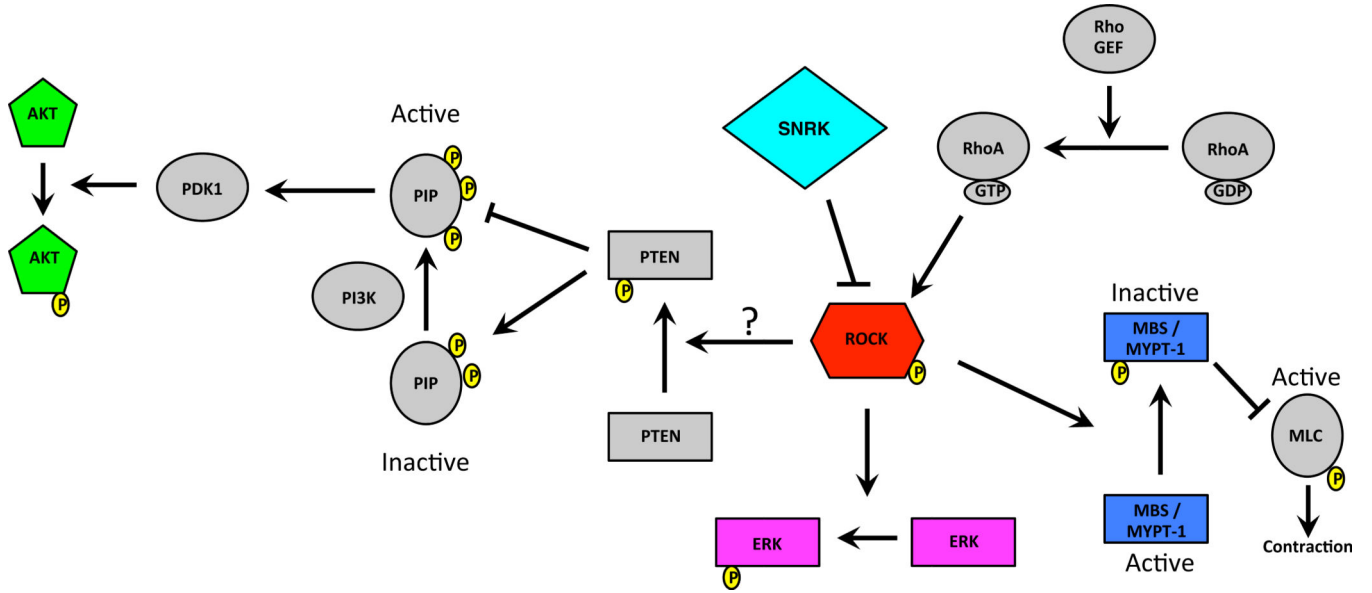


Figure 6. Proposed model for the mechanism of SNRK regulation of ROCK activity. ROCK is a major downstream effector of the small GTPase RhoA. Upon activation, ROCK can influence cellular contraction by phosphorylating myosin-binding subunit (MBS, also known as MYPT-1) of the myosin phosphatase complex. Phosphorylation of the myosin phosphatase complex renders the complex inactive and it is no longer able to remove the active phosphate group from phosphorylated myosin light chain (pMLC). Phosphorylated MLC is active and able to promote cellular contraction. SNRK regulates this process by modulating ROCK activity via phosphorylation of ROCK. ROCK can also influence ERK phosphorylation and nuclear localization as well as activate PTEN, which in turns inhibits the PI3K pathway resulting in the inhibition of phospho-AKT.